Am J Cancer Res 2024;14(5):2240-2252
www.ajcr.us /ISSN:2156-6976/ajcr0155266

Original Article

The transcriptomic expression pattern of immune checkpoints shows heterogeneity between and within cancer types

Hirotaka Miyashita[1*], Nicholas J Bevins[2*], Kartheeswaran Thangathurai[3,4], Suzanna Lee[5], Sarabjot Pabla[6], Mary K Nesline[6], Sean T Glenn[6,7], Jeffrey M Conroy[6,8], Paul DePietro[6], Eitan Rubin[3], Jason K Sicklick[9], Shumei Kato[5], Razelle Kurzrock[10]

[1]Department of Hematology and Oncology, Dartmouth Hitchcock Medical Center, Lebanon, NH, USA; [2]Department of Pathology, University of California San Diego, La Jolla, CA, USA; [3]The Shraga Segal Department for Microbiology, Immunology and Genetics, Ben-Gurion University of The Negev, Beer Sheva, Israel; [4]Department of Physical Science, University of Vavuniya, Vavuniya, Sri Lanka; [5]Center for Personalized Cancer Therapy and Division of Hematology and Oncology, Department of Medicine, UC San Diego Moores Cancer Center, La Jolla, CA, USA; [6]OmniSeq Inc., Buffalo, NY, USA; [7]Roswell Park Comprehensive Cancer Center, Molecular Pathology, Buffalo, NY, USA; [8]Roswell Park Comprehensive Cancer Center, Center for Personalized Medicine, Buffalo, NY, USA; [9]Division of Surgical Oncology, Department of Surgery and Center for Personalized Cancer Therapy, University of California, San Diego, La Jolla, CA, USA; [10]Worldwide Innovative Network (WIN) for Personalized Cancer Therapy, Paris, France. [*]Equal contributors.

Received January 3, 2024; Accepted April 11, 2024; Epub May 15, 2024; Published May 30, 2024

Abstract: Transcriptomic expression profiles of immune checkpoint markers are of interest in order to decipher the mechanisms of immunotherapy response and resistance. Overall, 514 patients with various solid tumors were retrospectively analyzed in this study. The RNA expression levels of tumor checkpoint markers (ADORA2A, BTLA, CD276, CTLA4, IDO1, IDO2, LAG3, NOS2, PD-1, PD-L1, PD-L2, PVR, TIGIT, TIM3, VISTA, and VTCN) were ranked from 0-100 percentile based on a reference population. The expression of each checkpoint was correlated with cancer type, microsatellite instability (MSI), tumor mutational burden (TMB), and programmed death-ligand 1 (PD-L1) by immunohistochemistry (IHC). The cohort included 30 different tumor types, with colorectal cancer being the most common (27%). When RNA percentile rank values were categorized as "Low" (0-24), "Intermediate" (25-74), and "High" (75-100), each patient had a distinctive portfolio of the categorical expression of 16 checkpoint markers. Association between some checkpoint markers and cancer types were observed; NOS2 showed significantly higher expression in colorectal and stomach cancer ($P < 0.001$). Principal component analysis demonstrated no clear association between combined RNA expression patterns of 16 checkpoint markers and cancer types, TMB, MSI or PD-L1 IHC. Immune checkpoint RNA expression varies from patient to patient, both within and between tumor types, though colorectal and stomach cancer showed the highest levels of NOS2, a mediator of inflammation and immunosuppression. There were no specific combined expression patterns correlated with MSI, TMB or PD-L1 IHC. Next generation immunotherapy trials may benefit from individual analysis of patient tumors as selection criteria for specific immunomodulatory approaches.

Keywords: Immune checkpoint, transcriptome, principal component analysis, microsatellite instability, tumor mutational burden, programmed death ligand 1

Introduction

Concerted efforts to activate the immune system against cancers, including with the use of cytokines, vaccines, cellular therapy, and checkpoint blockade, have led to regulatory approval of several immunotherapeutic medications. In particular, the discovery of the molecular mechanisms of immune suppression in the tumor microenvironment resulted in the utilization of more potent immunotherapy, which has revolutionized the field of medical oncology. The first immune checkpoint blockade (ICB) approved by Food and Drug Ad-

https://doi.org/10.62347/JRJP7877

ministration (FDA) was ipilimumab, a monoclonal antibody targeting cytotoxic T-lymphocyte-associated protein 4 (CTLA-4), for advanced melanoma [1]. As of 2022, FDA has approved one CTLA-4 inhibitor, four programmed death 1 (PD-1) inhibitors, three programmed death-ligand 1 (PD-L1) inhibitors [2-4], and a lymphocyte-activation gene 3 (LAG3) inhibitor [5].

Although ICBs have been improving cancer treatment outcomes, not all patients with cancer benefit from them. Overcoming the limitation of non-responders has been a challenge, which has led to the discovery of several response markers to ICBs, including but not limited to PD-L1 expression status [6, 7], microsatellite instability (MSI) [8], tumor mutational burden, and more recently PD-1 expression on tumor infiltrating lymphocytes [9-12]. In recent years, several genomic mutations (e.g., *ARID1A* mutation) have been shown to be associated with favorable responses to ICBs [13-16]. On the other hand, several markers that are potentially related to ICB resistance have been studied, including but not limited to *EGFR* mutation [17], *MDM2* amplification [18], Wnt-beta catenin activation [19], and alterations of beta-2 microglobulin [20]. These markers can potentially help predict patients to whom ICBs should or should not be given. The study of the predictive markers is not limited to genomics or protein expression. We also previously reported that high ribonucleic acid (RNA) expression level of T cell immunoglobulin and mucin domain-containing protein 3 (TIM3) and V-domain Ig suppressor of T cell activation (VISTA) checkpoints correlate with poor response to ICBs [21]. The latter suggests that there may be evasion pathways other than the PD-1/PD-L1 axis that protect tumors from immune eradication.

Selecting patients to receive specific ICBs based on genomic alterations (e.g., mismatch repair gene defect) or expression levels of a specific protein (e.g., PD-L1) has become a routine practice in several types of cancer [22]. Another step can be analyzing the immunomic profile to determine the precise mechanism an individual cancer is using to inactivate and elude the immune apparatus. However, our understanding of the immunome in various types of cancer is still limited. Therefore, we analyzed the transcriptomic expression of multiple immune checkpoints among diverse cancers. Our hypothesis was that immune checkpoint expression will demonstrate heterogeneity, which in turn may be informative when selecting treatments. Herein, we showed that RNA expression of immune checkpoints varies between patients, both within and between tumor types, suggesting the need to interrogate each tumor to properly select therapy in a precision immunotherapy paradigm.

Materials and methods

Patients

As a retrospective part of Study of Personalized Cancer Therapy to Determine Response and Toxicity (UCSD_PREDICT, NCT02478931), 514 patients with various types of solid tumors seen at the Center for Personalized Cancer Therapy within Moores Cancer Center at UC San Diego were included in this study. The RNA expression levels of immune checkpoint inhibitory markers in these patients' samples were measured at a Clinical Laboratory Improvement Amendments (CLIA)-licensed and College of American Pathologist (CAP)-accredited clinical laboratory, OmniSeq (https://www.omniseq.com/). The patient characteristic data, including age, sex, the origin of cancer, MSI, TMB and the expression of PD-L1 by immunohistochemistry (IHC), were collected. When one patient had two or more samples from different collection dates, the sample collected earliest was used for the analysis. We followed the guidelines of the UCSD Institutional Review Board for data collection (UCSD_PREDICT, NCT02478931) and any investigational interventions for which patients consented.

Tissue sampling and the analysis of RNA expression

After collection, tissues were processed as formalin-fixed, paraffin-embedded (FFPE) samples and analyzed through RNA sequence at OmniSeq laboratory. RNA was extracted from FFPE using truXTRAC FFPE extraction kit (Covaris, Inc., Woburn, MA), with slight modification complying with the manufacturer's instruction. After RNA was purified from the sample, it was dissolved in 50 μL water, and the yield was analyzed through Quant-iT RNA HS assay (Thermo Fisher Scientific, Waltham, MA). The pre-defined titer of 10 ng RNA was

set as acceptance criteria so that the library was prepared appropriately. Absolute reading of the RNA sequence was measured by Torrent Suite's plugin immuneResponseRNA (v5.2.0.0). The RNA expression of a total of 397 different genes was measured. Among them, 16 genes related to the immune checkpoint, including ADORA2A, BTLA, CD276, CTLA4, IDO1, IDO2, LAG3, NOS2, PD-1, PD-L1, PD-L2, PVR, TIGIT, TIM3, VISTA, and VTCN were focused on this study (Supplementary Table 1). The expression level of RNA was normalized to internal housekeeping gene profiles and ranked (0-100 percentile) in a standardized manner to a reference population of 735 tumors with 35 different histologies. The RNA expression profiles were categorized by rank values into "Low" (0-24 percentile), "Intermediate" (25-74 percentile), and "High" (75-100 percentile).

Definition of TMB, MSI and PD-L1 status

As for TMB, genomic DNA was extracted from qualified FFPE tumor samples (> 30% neoplastic nuclei) using the truXTRAC FFPE extraction kit (Covaris) with 10 ng DNA input for the library preparation. Ion AmpliSeq targeted sequencing chemistry with Comprehensive Cancer Panel was used for DNA library preparation, followed by the enrichment and template preparation using the Ion Chef System and sequencing on the Ion S5XL 540 chip (Thermo Fisher Scientific). After removal of germline variants, synonymous variants, indels, and single nucleotide variants (SNVs) with < 5% variant allele fraction (VAF), TMB was reported as eligible mutations per qualified panel size (mutations/megabase). In this analysis, TMB ≥ 10 mutations per megabase was designated as TMB "High" and less than 10 mutations per megabase was defined as TMB "Low".

To determine MSI, genomic DNA was extracted from qualified FFPE samples (> 20% neoplastic nuclei) by truXTRAC FFPE extraction kit (Covaris). The MSI - next-generation sequencing (NGS) assay analyzes 29 homopolymer loci, including BAT-25 and BAT-26, by running sequencing tumor DNA (20 ng) on an Illumina MiSeq Sequencer. The computational tool of the assay, MSI-NGS Caller, compares the sample's homopolymer repeat profile to a normal allele distribution that was predefined at each locus.

PD-L1 expression was measured by three different IHC assays; VENTANA PD-L1 (SP 142) assay (Ventana Medical Systems, Inc., Tuscon, Arizona, USA, N = 33), Dako PD-L1 IHC 22C3 pharmDx assay, and Dako PD-L1 IHC 288 pharmDx assay (Dako North America, Inc., Carpinteria, California, USA, N = 474 and 6, respectively). In this analysis, positive PD-L1 in IHC was determined by PD-L1 ≥ 1%, and otherwise, the samples were classified as negative PD-L1.

Statistical analysis

The characteristics of the patients included in the study and the expression of immune checkpoint markers were summarized by the descriptive statistics. The correlation between each immune checkpoint expression and other variables, including cancer types, TMB, MSI, and PD-L1, were analyzed through the Kruskal-Wallis test.

The correlation between expression patterns of immune checkpoint markers and other variables was analyzed through principal component analysis and was quantified by silhouette scores.

All statistical analysis was conducted through R 3.6.1 (R Foundation for Statistics Computing, Vienna, Austria) and was confirmed by a statistician and bioinformatician. R packages "ggplot2", "dplyr", "tidyr", "stringr", "tidyverse", "cluster", "factoextra", and "dendextend" were used in this analysis. Statistical significance was determined as $P < 0.05$ with the Bonferroni correction for multiple comparisons.

Results

Characteristics of the cohort

Altogether, 514 patients with advanced/metastatic disease were included, and the analysis was done between July 2017 and November 2020. 310 patients (60.3%) were women; the patients' age ranged from 23 to 93 years (median = 60 years). The most common type of cancer was colorectal cancer (N = 140, 27.2%), followed by pancreatic cancer (N = 55, 10.7%) and breast cancer (N = 49, 9.5%). Overall, 450 and 440 patients had samples available for the analysis of TMB and MSI,

Table 1. Patients' baseline characteristics

	Entire cohort (N = 514)		TMB (N = 450)		MSI (N = 440)	
	Number of patients with data	%	Number of patients with data	%	Number of patients with data	%
Sex						
Female	310	60.3	273	60.7	272	61.8
Male	204	39.7	177	39.3	168	38.2
Age (years)						
-49	124	24.1	111	24.7	109	24.8
50-59	121	23.5	105	23.3	102	23.2
60-69	146	28.4	127	28.2	129	29.3
70-	123	23.9	107	23.8	100	22.7
Cancer Type						
Colorectal	140	27.2	120	26.7	130	29.5
Pancreatic	55	10.7	43	9.6	47	10.7
Breast	49	9.5	46	10.2	42	9.5
Ovarian	43	8.4	41	9.1	35	8.0
Stomach	25	4.9	22	4.9	19	4.3
Sarcoma	24	4.7	23	5.1	21	4.8
Uterine	24	4.7	21	4.7	21	4.8
Lung	20	3.9	17	3.8	15	3.4
Liver and Bile duct	19	3.7	13	2.9	14	3.2
Esophageal	17	3.3	15	3.3	15	3.4
Neuroendocrine	15	2.9	15	3.3	14	3.2
Unknown primary	13	2.5	12	2.7	10	2.3
Head and Neck	12	2.3	12	2.7	11	2.5
Small intestine	12	2.3	9	2.0	8	1.8
Melanoma	6	1.2	6	1.3	6	1.4
Others	40	7.8	35	7.8	32	7.3

Others in the entire cohort include: cervical cancer (N = 5), bladder cancer (N = 4), gallbladder and extrahepatic bile duct cancers (N = 4), prostate cancer (N = 4), brain and nervous system cancers (N = 3), kidney and renal pelvis cancers (N = 3), squamous cell carcinoma of the skin (N = 3), thyroid cancer (N = 3), adrenal gland cancer (N = 3), lipomatous neoplasm (N = 2), mesothelioma (N = 2), basal cell carcinoma of the skin (N = 1), ocular melanoma (N = 1), primary peritoneal carcinoma (N = 1), and thymic cancer (N = 1). Abbreviations: MSI: microsatellite instability, TMB: tumor mutational burden.

respectively. The distribution of baseline characteristics was similar in all cohorts (**Table 1**).

Transcriptomic expression of checkpoint markers demonstrates a distinct pattern of expression in each patient

In the original cohort, the RNA rank values of each immune checkpoint marker were widely distributed from 0-99 or 0-100. The median rank values of each checkpoint marker ranged from 13.5 (NOS2) to 68 (CD276 (B7-H3)) (**Figure 1A**).

CD276 (B7-H3) showed high RNA expression level (rank value of 75 or higher) most frequently among the 16 checkpoint markers (N = 214, 41.6%) and PD-L1 had the lowest proportion of high expression (N = 67, 13%). The proportion of low expression (rank value of 24 or lower) ranged from 11.9% (CD276 (B7-H3), N = 61) to 52.5% (NOS2, N = 270) (**Figure 1B**).

Among 514 patients in this study, each patient had distinctive patterns of expression levels of 16 checkpoint inhibitor markers (**Figure 2**).

RNA expression of checkpoint markers according to cancer types

Although the expression patterns of the checkpoint markers were extremely diverse (**Figure 2**), the expression of some checkpoint markers was significantly associated with cancer types. For instance, NOS2 showed the greatest difference in RNA expression depending on cancer

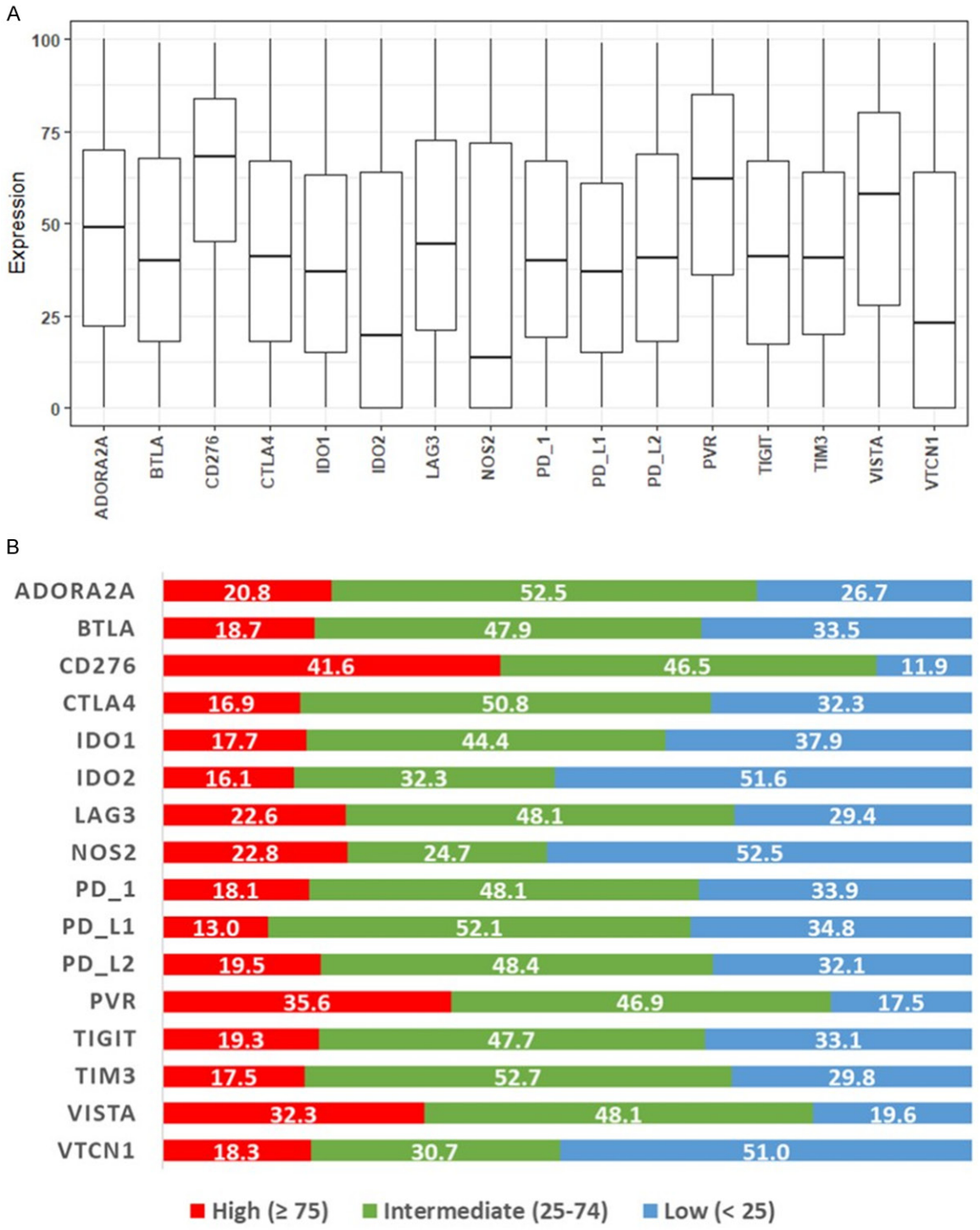

Figure 1. RNA expression of immune checkpoint markers (N = 514 patients with diverse cancers). A. Box plot of immune checkpoint marker RNA expression. Each box represents the middle 50% of scores for the group. The bottom of the box represents the first quartile, and the top represents the third quartile. The thick line dividing the box into two parts represents the median. The upper and lower whiskers extend to the largest value but are no further than 1.5 times of the inter-quartile range from the third quartile. All markers demonstrated the range of rank value (transcript expression rank as compared to control (see Methods)) from 0 to 100 percentile. The median rank values of each checkpoint marker ranged from 13.5 percentile (NOS2) to 68 percentile (CD276 (B7-H3)). B. Bar chart of the immune checkpoint marker RNA expression category. The numbers in the bars represent the percentage of patients who had high (≥ 75), intermediate (25-74), and low (< 25) rank RNA percentile expression of each checkpoint marker. For example, 20.8% (N = 107) of patients in the entire cohort had high RNA expression of ADORA2A.

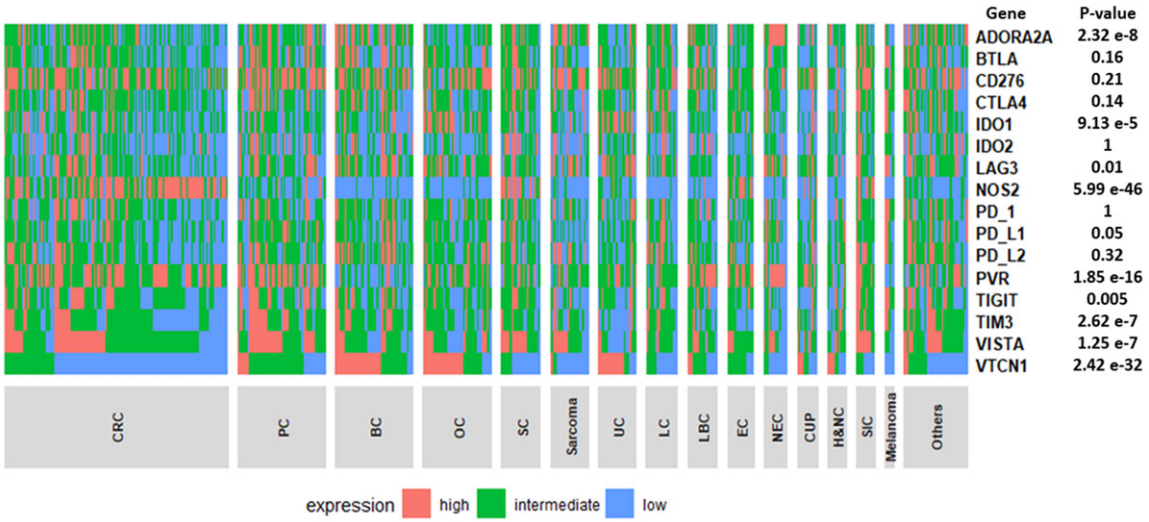

Figure 2. Heatmap of RNA expression levels of immune checkpoint markers in the entire cohort. The RNA level of expression is classified by the color. Red means high RNA expression (≥ 75 rank percentile). Green demonstrates intermediate RNA expression (25-74 rank percentile), and low RNA expression (< 25 rank percentile) was marked by the blue. *P*-values were calculated by the Kruskal-Wallis test with Bonferroni correction for the multiple comparisons for the 16 genes. Abbreviations: BC: breast cancer, CRC: colorectal cancer, CUP: cancer of unknown primary, EC: esophageal cancer, H&NC: head and neck cancer, LBC: liver and bile duct cancer, LC: lung cancer, NEC: neuroendocrine cancer, OC: ovarian cancer, PC: pancreatic cancer, SC: stomach cancer, SIC: small intestine cancer, UC: uterine cancer.

types (P < 0.001) (**Figure 3A**); the median rank values of NOS2 in colorectal, pancreatic, breast, and stomach cancer were 79, 5, 0, and 76 percentile, respectively. IDO2 showed the least difference in RNA expression levels across cancer types (**Figure 3B**, P = 1). A significant association between expression levels and cancer types was also seen in ADORA2A, IDO1, LAG3, PD-L1, PVR, TIGIT, TIM3, VISTA, and VTCN1 (Supplementary Figure 1).

Analyzing combined RNA expression patterns of 16 checkpoint markers shows no clear correlation with cancer types

The immune checkpoint markers of the 514 tumors were analyzed for the correspondence with cancer types. The 514 samples were plotted using principal component analysis for the selected 16 genes and were clustered based on their cancer types (**Figure 4**). Principal component analysis allows 2D representation of 16-dimensional data consisting of expression levels of 16 different genes [23]. Among the clusters, 16 small clusters (i.e., clusters size is smaller than the median cluster size, n = 4) were omitted, resulting in removal of 36. The first dimension ("Dim1") captured 38.4% of the variation in the data, and the second dimension ("Dim2") captured 10.8% of variation in the data. The plot did not show a clear distinction between different tissues in the expression of the 16 checkpoint markers.

To quantify these differences, we compared the silhouette score with and without randomization. Silhouette score quantifies the average variation within clusters compared to the variation between clusters [24]. This measure can be used to compare actual and shuffled tumor types as clusters, and to calculate its average and standard deviation. The silhouette score of the non-randomized cancer types was -0.08 and the silhouette score of 100000 randomizations was 0.1 ± 0.015 (Supplementary Table 2), which suggests that cancer types are not significantly correlated with checkpoint RNA expression pattern.

Correlation between the expression of checkpoint markers and other molecular characteristics

Comparing the expression of each checkpoint marker based on TMB status, no significant difference was detected (**Figure 5A**). The expressions of several checkpoint markers, including IDO1, PD-L1, and TIGIT, were associated with

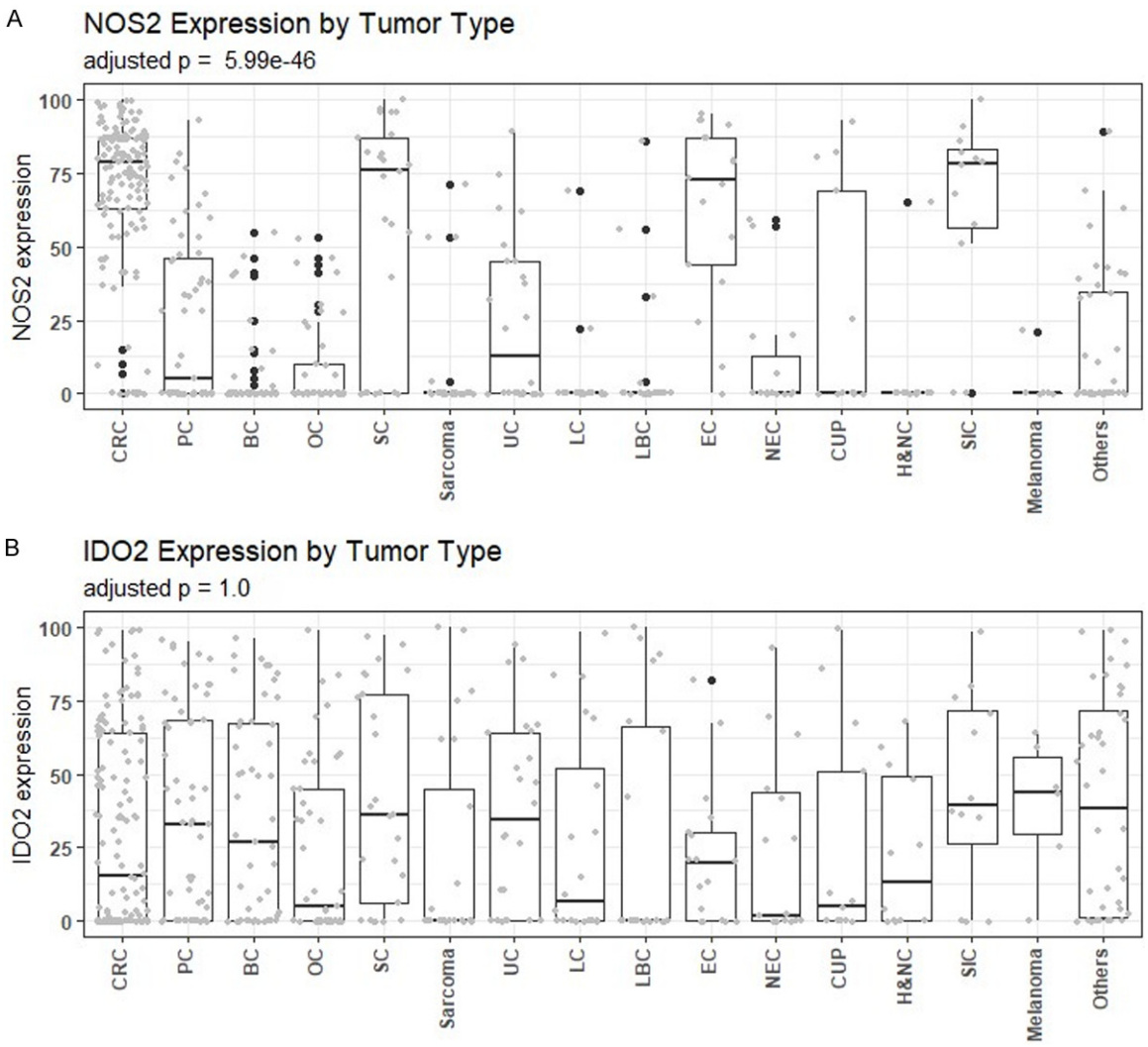

Figure 3. Box plots for the RNA expression of checkpoint markers. NOS2 (A) and IDO2 (B) were chosen for depiction because NOS2 represented most significant differences between cancer types and IDO2 expression levels represented the least significant differences between cancer types. See also **Figure 2**. Each box represents the middle 50% of scores for the group. The bottom of the box represents the first quartile, and the top represents the third quartile. The thick line dividing the box into two parts means the median. The upper whisker extends to the largest value no further than 1.5 times of inter-quartile range from the third quartile. The lower whisker extends to the smallest value no further than 1.5 times of inter-quartile range from the first quartile. Any values outside the scope of the box and the whiskers are regarded as outliers and demonstrated by solid dots. Gray dots represent all values in the entire cohort. *P*-values were calculated by the Kruskal-Wallis test with Bonferroni correction for the multiple comparisons for the 16 genes. While IDO2 showed no difference in expression level between cancer types, NOS2 demonstrated significant RNA expression differences as shown. See also Supplementary Figure 1 for differences in cancer type expression and other checkpoints. Abbreviations: BC: breast cancer, CRC: colorectal cancer, CUP: cancer of unknown primary, EC: esophageal cancer, H&NC: head and neck cancer, LBC: liver and bile duct cancer, LC: lung cancer, NEC: neuroendocrine cancer, OC: ovarian cancer, PC: pancreatic cancer, SC: stomach cancer, SIC: small intestine cancer, UC: uterine cancer.

MSI (**Figure 5B**). The expression of PD-L1 was significantly higher in the patients with MSI than in those with stable microsatellites (median rank value 68 and 37, respectively, P = 0.005). Similarly, PD-L1 expression equal or greater than 1% on IHC showed associations with the higher RNA expression of CTLA4, IDO1, LAG3, PD-1, PD-L1, PD-L2, and TIGIT (**Figure 5C**). The RNA of PD-L1 was significantly more highly expressed in the tumors with PD-L1 positivity in IHC (≥ 1%) than those with negative PD-L1 in IHC (< 1%) (median rank value 53 and

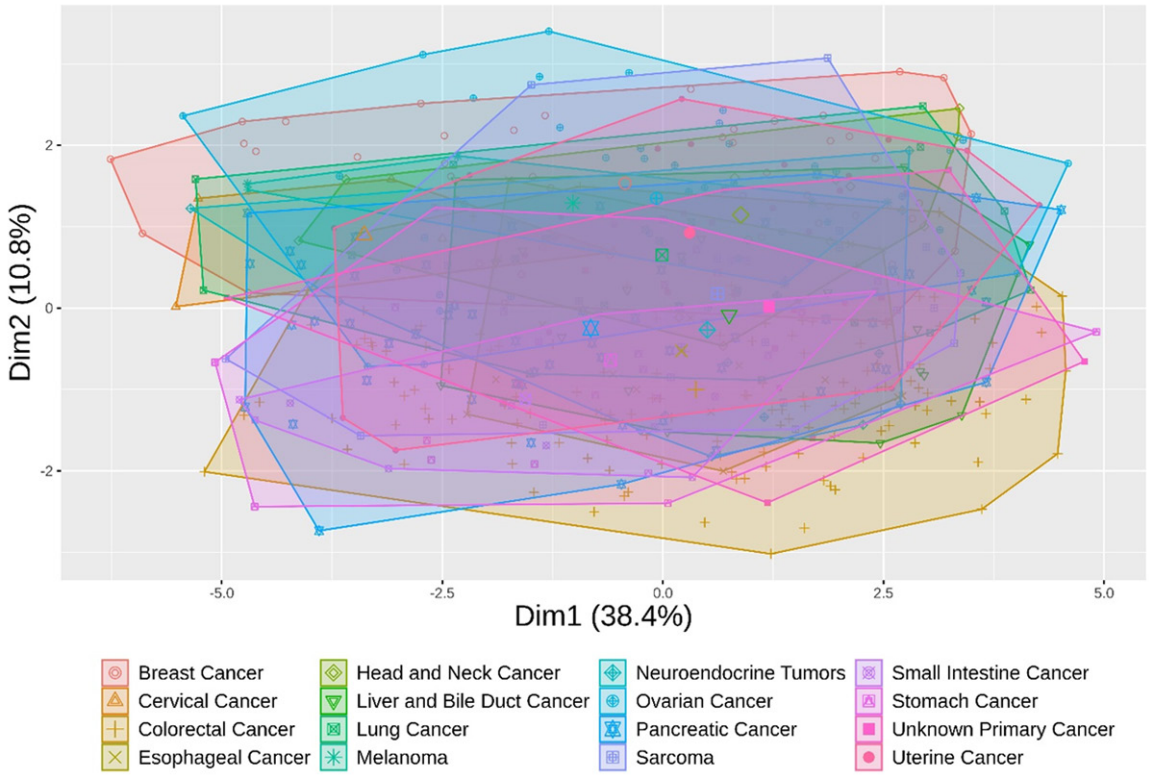

Figure 4. The cluster of plots of dataset with 514 tumors for the selected 16 checkpoint RNA expression based on cancer type using principal component analysis (See methods and Supplementary Tables 1 and 2). The cluster of plots of dataset with 514 tumors for the selected 16 checkpoint genes (see Supplementary Table 1) which were assessed for RNA expression level based on cancer type using principal component analysis. The cluster assignment is made based on its cancer type. Among the clusters, 16 small clusters (i.e., clusters size is smaller than the median cluster size, n = 4) of cancer type were omitted, resulting in removal of 36 samples (of a total of 514). To test this prediction, we first use principal component analysis to allow 2D representation of 16-dimensional data (considering each gene a dimension). The first dimension ("Dim1") captured 38.4% of the variation in the data, and the second dimension ("Dim2") captured 10.8% of variation in the data. Examining the distribution of values in the 1st and 2nd dimensions with each tissue type shown in a distinct color. From this plot, and the calculated values in Supplementary Table 2, it does not seem that there is a clear distinction between different tissues in the expression of the 16 checkpoint genes.

31, respectively, $P < 0.001$). Despite the correlation between MSI or PD-L1 and several individual checkpoints, when analyzed together, the principal component analysis plots with the clustering based on MSI, TMB as well as PD-L1 IHC showed no apparent correlation with the patterns of checkpoint marker expression (Supplementary Figure 2).

Discussion

This analysis showed that the expression levels of checkpoint markers are extremely diverse among cancers. There was no single identical expression pattern of 16 checkpoint markers shared by multiple samples in this cohort of 514 patients with cancer. However, when focusing on the expression level of each checkpoint marker, a significant association between cancer types and the expression levels was observed.

Inducible nitric oxide synthase (NOS2) is known to play a role in immunosuppression in microenvironments of cancer, and its overexpression is related to poor outcomes in various types of cancer [25]. We revealed that NOS2 is highly expressed in colorectal and stomach cancer, while pancreatic and breast cancer demonstrated a low expression level of NOS2. It has been suggested that NOS2 contributes to the carcinogenesis and progression of gastrointestinal cancers, including colorectal, gastric, and esophageal cancer, which is compatible with

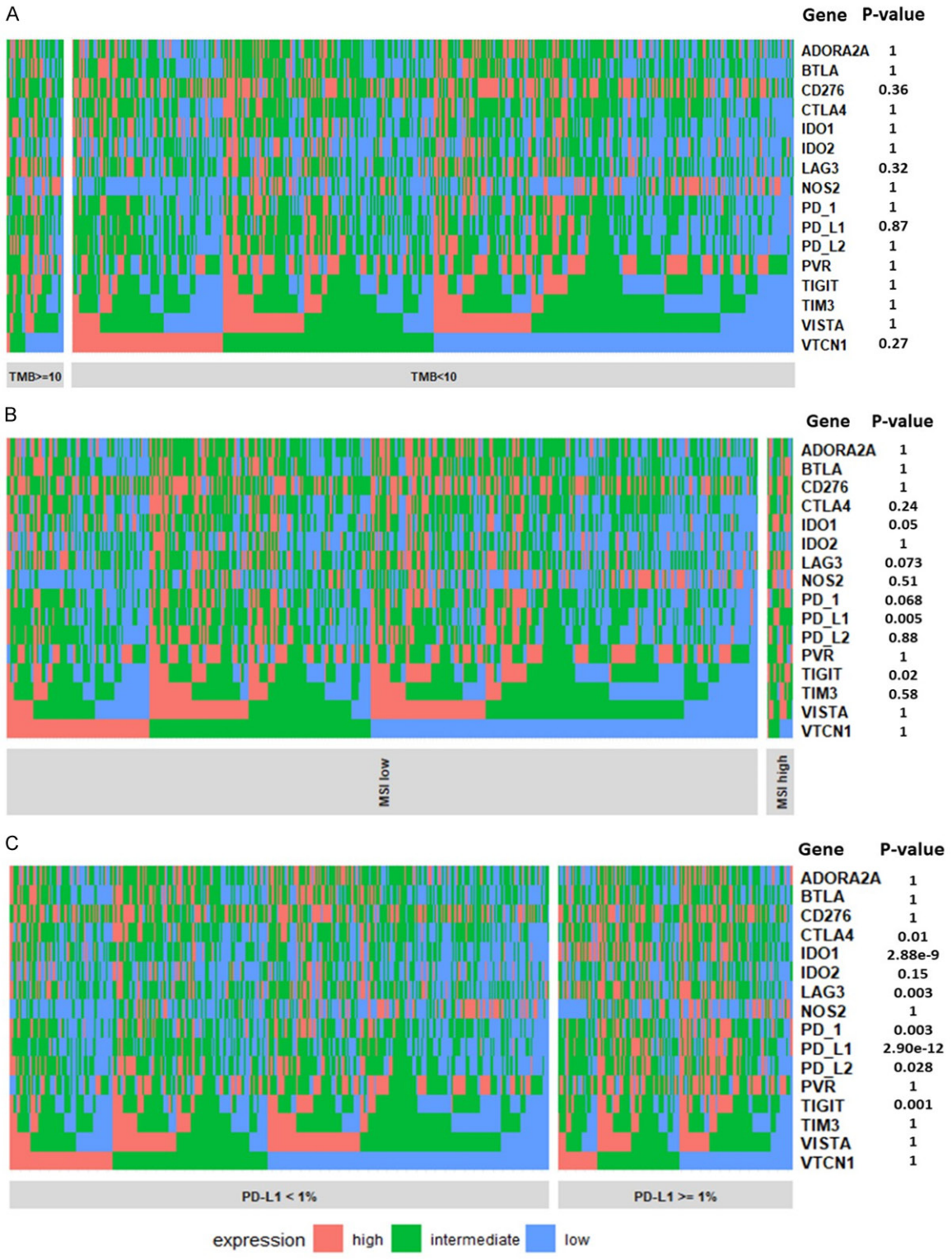

Figure 5. Heatmaps of expression levels of checkpoint markers based on TMB, MSI, and PD-L1 IHC. The expression levels of checkpoint markers are summarized in the heatmaps based on TMB (A), MSI (B) and PD-L1 IHC (C). The level of expression is classified by the color. Red means high RNA expression (≥ 75 percentile rank). Green demonstrates intermediate expression (25-74), and low expression (< 25) was marked by the blue. *P*-values were calculated by the Kruskal-Wallis test with Bonferroni correction for the multiple comparisons for the 16 genes. These figure show that higher RNA level of CTLA4, LAG3, PD-1, PD-L1, PD-L2 and TIGIT are significantly associated with PD-L1 greater or equal to 1% on IHC. Abbreviations: IHC: immunohistochemistry, MSI: microsatellite instability, PD-L1: programmed death-ligand 1 (immunohistochemistry), TMB: tumor mutational burden.

the result of this analysis [26]. Since NOS2 can theoretically bring about a poor response to immunotherapy of cancer, inhibiting NOS2 may be a promising approach to enhance immunotherapy efficacy in certain types of cancer that show high NOS2 expression [27].

Our analysis demonstrated that poliovirus receptor (PVR) is also relatively highly expressed in colorectal and pancreatic cancer, while breast cancer and melanoma generally express PVR in the lower levels. It has been shown that PVR is involved in immune regulation in cancer and is deemed an attractive target for cancer immunotherapy [28]. PVR is expressed on the membrane of various cancer cells and serves as a ligand of TIGIT, whose interaction causes an immunosuppressive effect [29]. Thus PVR is thought to be a promising target for cancer immunotherapy [30]. It has been reported that PVR is highly expressed in various types of cancers and cell lines [31], but no previous report comprehensively compared different cancer types for the expression level of PVR using human samples. To our best knowledge, there is no ongoing trial directly targeting PVR as a cancer treatment [32], but the difference in expression of PVR among different cancer types should be considered when clinical trials focusing on PCR blockade are designed.

In this analysis, V-set domain-containing T-cell activation inhibitor 1 (VTCN1) was highly expressed in breast, ovarian and uterine cancer, while its expression level was relatively lower in gastrointestinal cancer such as colorectal or gastric cancer. VTCN1 is known to be expressed in several types of cancers, including gastric, ovarian, and renal cancer [33]. While there are contradictory data regarding the role of VTCN1 in anti-cancer immunity [34, 35], inhibition of VTCN1 through monoclonal antibody was proven to lead to anti-tumor immunity in mice [36]. Given that VTCN1 is also a good candidate to be targeted in cancer immunotherapy, knowing the different expression levels in each cancer type should be of interest.

Although ICB through the PD-1/PD-L1 axis has revolutionized the medical treatment of cancer, a substantial portion of cancer patients does not respond to currently available immunotherapies [37]. Cancer immunity is a complex process, where the PD-1/PD-L1 axis contributes only partially. Many other molecules, including TIGIT, LAG3, TIM3, and VISTA, also play essential roles in the immune checkpoint, which explains the limited efficacy of monotherapy of PD-1 or PD-L1 inhibition [38]. Therefore, a comprehensive analysis of the molecules involved in the immune checkpoint in cancer is pivotal to enhance the efficacy of already available and newly investigated ICBs. The efficacy of relatlimab, a LAG-3 inhibitor, has been reported, which will eventually shed light on the combination of ICBs targeting multiple axes [39].

In this analysis, each checkpoint marker demonstrated distinct expression levels in different types of cancer. However, when we tried to capture the pattern of all checkpoint marker expression through principal component analysis, there was no distinctive expression pattern based on cancer types or other molecular characteristics such as PD-L1, TMB, or MSI. As PD-1/PD-L1 inhibitors shows more benefit in patients with high PD-1 and PD-L1 expression in certain types of cancers [2, 12], inhibitors of another axis are expected to be more effective in cancers with high target molecule expression. Therefore, it may be reasonable to design a clinical trial of a new therapeutic targeting an immune checkpoint molecule by examining expression level of that molecule in the tumors of potential patients, reflecting a precision immunotherapy approach.

Due to the complexity of cancer immunity, the 16 genes analyzed in this study may not fully represent immunomic status. Additionally, the number of patients with some cancer types was limited. Further exploration of prognostic and predictive implications of immunomic heterogeneity is warranted. Finally, this was a single center study; future investigation of samples from multiple centers may be worthwhile.

In conclusion, we demonstrate the diversity and heterogeneity in immune checkpoint marker expression among various types of cancer. Although the expression of some markers was correlated with cancer type and molecular features, overall, there was patient-to-patient variability between and within cancer types. This finding suggests the need for molecular interrogation of every patient in order to maximize the efficacy of already available and currently investigated therapeutics, consistent with a personalized immunotherapy strategy.

Acknowledgements

This study was funded in part by the NIH P30 CA023100 (SK).

We followed any investigational interventions for which patients consented.

Disclosure of conflict of interest

Nicholas J Bevins serves as clinical laboratory director for Bertis Biosciences Inc., Birdrock Laboratory, and COVx laboratory. Nicholas J Bevins serves as Chief Medical Officer of Sequence Sciences. Sarabjot Pabla is/was an employee of OmniSeq and declares the following relationships: stock ownership from Labcorp. Mary K Nesline is/was an employee of OmniSeq and declares the following relationships: stock ownership from Labcorp. Sean T Glenn is/was an employee of OmniSeq and declares the following relationships: None. Jeffrey M Conroy is/was an employee of OmniSeq and declares the following relationships: stock ownership from Labcorp. Paul DePietro is/was an employee of OmniSeq and declares the following relationships: stock ownership from Labcorp. Jason K Sicklick receives consultant fees from Deciphera, Aadi and Grand Rounds; serves as a consultant for CureMatch, received speakers fees from Deciphera, La-Hoffman Roche, Foundation Medicine, Merck, QED and Daiichi Sankyo; and owns stock in Personalis. Shumei Kato serves as a consultant for Medpace, Foundation Medicine, NeoGenomics and CureMatch. He receives speaker's fee from Roche/Genentech and Bayer, and advisory board for Pfizer. He has research funding from ACT Genomics, Sysmex, Konica Minolta, OmniSeq, Personalis and Function Oncology. Razelle Kurzrock has received research funding from Biological Dynamics, Boehringer Ingelheim, Debiopharm, Foundation Medicine, Genentech, Grifols, Guardant, Incyte, Konica Minolta, Medimmune, Merck Serono, Omniseq, Pfizer, Sequenom, Takeda, and TopAlliance; as well as consultant and/or speaker fees and/or advisory board for Actuate Therapeutics, AstraZeneca, Bicara Therapeutics, Biological Dynamics, Caris, Daiichi Sankyo, Inc., Datar Cancer Genetics, EISAI, EOM Pharmaceuticals, Ilylon, Merck, NeoGenomics, Neomed, Pfizer, Prosperdtx, Roche, TD2/Volastra, Turning Point Therapeutics, X-Biotech; has an equity interest in CureMatch Inc., CureMetrix, and IDbyDNA; serves on the Board of CureMatch and CureMetrix, and is a co-founder of CureMatch.

Address correspondence to: Dr. Hirotaka Miyashita, Department of Hematology and Oncology, Dartmouth Cancer Center, 1 Medical Center Drive, Lebanon, NH 03766, USA. Tel: 603-650-4344; E-mail: miyashita.hirotaka@gmail.com; Dr. Shumei Kato, Center for Personalized Cancer Therapy and Division of Hematology and Oncology, Department of Medicine, UC San Diego Moores Cancer Center, 3855 Health Sciences Drive, La Jolla, CA 92093, USA. Tel: 858-822-2372; Fax: 858-822-6186; E-mail: smkato@health.ucsd.edu; Dr. Razelle Kurzrock, Worldwide Innovative Network (WIN) Consortium for Precision Medicine, Paris, France. E-mail: teoam2011@gmail.com

References

[1] Hodi FS, O'Day SJ, McDermott DF, Weber RW, Sosman JA, Haanen JB, Gonzalez R, Robert C, Schadendorf D, Hassel JC, Akerley W, van den Eertwegh AJ, Lutzky J, Lorigan P, Vaubel JM, Linette GP, Hogg D, Ottensmeier CH, Lebbé C, Peschel C, Quirt I, Clark JI, Wolchok JD, Weber JS, Tian J, Yellin MJ, Nichol GM, Hoos A and Urba WJ. Improved survival with ipilimumab in patients with metastatic melanoma. N Engl J Med 2010; 363: 711-23.

[2] Vaddepally RK, Kharel P, Pandey R, Garje R and Chandra AB. Review of indications of FDA-approved immune checkpoint inhibitors per NCCN guidelines with the level of evidence. Cancers (Basel) 2020; 12: 738.

[3] Kasherman L, Ahrari S and Lheureux S. Dostarlimab in the treatment of recurrent or primary advanced endometrial cancer. Future Oncol 2021; 17: 877-92.

[4] Jardim DL, de Melo Gagliato D, Giles FJ and Kurzrock R. Analysis of drug development paradigms for immune checkpoint inhibitors. Clin Cancer Res 2018; 24: 1785-94.

[5] Paik J. Nivolumab Plus Relatlimab: first approval. Drugs 2022; 82: 925-931.

[6] Reck M, Rodríguez-Abreu D, Robinson AG, Hui R, Csőszi T, Fülöp A, Gottfried M, Peled N, Tafreshi A, Cuffe S, O'Brien M, Rao S, Hotta K, Leiby MA, Lubiniecki GM, Shentu Y, Rangwala R and Brahmer JR; KEYNOTE-024 Investigators. Pembrolizumab versus chemotherapy for PD-L1-positive non-small-cell lung cancer. N Engl J Med 2016; 375: 1823-33.

[7] Patel SP and Kurzrock R. PD-L1 expression as a predictive biomarker in cancer immunotherapy. Mol Cancer Ther 2015; 14: 847-56.

[8] André T, Shiu KK, Kim TW, Jensen BV, Jensen LH, Punt C, Smith D, Garcia-Carbonero R,

Benavides M, Gibbs P, de la Fouchardiere C, Rivera F, Elez E, Bendell J, Le DT, Yoshino T, Van Cutsem E, Yang P, Farooqui MZH, Marinello P and Diaz LA Jr; KEYNOTE-177 Investigators. Pembrolizumab in microsatellite-instability-high advanced colorectal cancer. N Engl J Med 2020; 383: 2207-18.

[9] Goodman AM, Kato S, Bazhenova L, Patel SP, Frampton GM, Miller V, Stephens PJ, Daniels GA and Kurzrock R. Tumor mutational burden as an independent predictor of response to immunotherapy in diverse cancers. Mol Cancer Ther 2017; 16: 2598-608.

[10] Jardim DL, Goodman A, de Melo Gagliato D and Kurzrock R. The challenges of tumor mutational burden as an immunotherapy biomarker. Cancer Cell 2021; 39: 154-73.

[11] Subbiah V, Solit DB, Chan TA and Kurzrock R. The FDA approval of pembrolizumab for adult and pediatric patients with tumor mutational burden (TMB) ≥10: a decision centered on empowering patients and their physicians. Ann Oncol 2020; 31: 1115-8.

[12] Bevins NJ, Okamura R, Montesion M, Adashek JJ, Goodman AM and Kurzrock R. Tumor infiltrating lymphocyte expression of PD-1 predicts response to anti-PD-1/PD-L1 immunotherapy. J Immunother Precis Oncol 2022; 5: 90-7.

[13] Okamura R, Kato S, Lee S, Jimenez RE, Sicklick JK and Kurzrock R. ARID1A alterations function as a biomarker for longer progression-free survival after anti-PD-1/PD-L1 immunotherapy. J Immunother Cancer 2020; 8: e00438.

[14] Pham TV, Boichard A, Goodman A, Riviere P, Yeerna H, Tamayo P and Kurzrock R. Role of ultraviolet mutational signature versus tumor mutation burden in predicting response to immunotherapy. Mol Oncol 2020; 14: 1680-94.

[15] Boichard A, Pham TV, Yeerna H, Goodman A, Tamayo P, Lippman S, Frampton GM, Tsigelny IF and Kurzrock R. APOBEC-related mutagenesis and neo-peptide hydrophobicity: implications for response to immunotherapy. Oncoimmunology 2018; 8: 1550341.

[16] Boichard A, Tsigelny IF and Kurzrock R. High expression of PD-1 ligands is associated with kataegis mutational signature and APOBEC3 alterations. Oncoimmunology 2017; 6: e1284719.

[17] Proto C, Ferrara R, Signorelli D, Lo Russo G, Galli G, Imbimbo M, Prelaj A, Zilembo N, Ganzinelli M, Pallavicini LM, De Simone I, Colombo MP, Sica A, Torri V and Garassino MC. Choosing wisely first line immunotherapy in non-small cell lung cancer (NSCLC): what to add and what to leave out. Cancer Treat Rev 2019; 75: 39-51.

[18] Cabezón-Gutiérrez L, Custodio-Cabello S, Palka-Kotlowska M, Alonso-Viteri S and Khosravi-Shahi P. Biomarkers of immune checkpoint inhibitors in non-small cell lung cancer: beyond PD-L1. Clin Lung Cancer 2021; 22: 381-9.

[19] Zhou Y, Xu J, Luo H, Meng X, Chen M and Zhu D. Wnt signaling pathway in cancer immunotherapy. Cancer Lett 2022; 525: 84-96.

[20] Wang H, Liu B and Wei J. Beta2-microglobulin(B2M) in cancer immunotherapies: biological function, resistance and remedy. Cancer Lett 2021; 517: 96-104.

[21] Kato S, Okamura R, Kumaki Y, Ikeda S, Nikanjam M, Eskander R, Goodman A, Lee S, Glenn ST, Dressman D, Papanicolau-Sengos A, Lenzo FL, Morrison C and Kurzrock R. Expression of TIM3/VISTA checkpoints and the CD68 macrophage-associated marker correlates with anti-PD1/PDL1 resistance: implications of immunogram heterogeneity. Oncoimmunology 2020; 9: 1708065.

[22] Ettinger DS, Wood DE, Aisner DL, Akerley W, Bauman JR, Bharat A, Bruno DS, Chang JY, Chirieac LR, D'Amico TA, Dilling TJ, Dowell J, Gettinger S, Gubens MA, Hegde A, Hennon M, Lackner RP, Lanuti M, Leal TA, Lin J, Loo BW Jr, Lovly CM, Martins RG, Massarelli E, Morgensztern D, Ng T, Otterson GA, Patel SP, Riely GJ, Schild SE, Shapiro TA, Singh AP, Stevenson J, Tam A, Yanagawa J, Yang SC, Gregory KM and Hughes M. NCCN guidelines insights: non-small cell lung cancer, version 2.2021. J Natl Compr Canc Netw 2021; 19: 254-66.

[23] Jolliffe IT and Cadima J. Principal component analysis: a review and recent developments. Philos Trans A Math Phys Eng Sci 2016; 374: 20150202.

[24] Zhao S, Sun J, Shimizu K and Kadota K. Silhouette scores for arbitrary defined groups in gene expression data and insights into differential expression results. Biol Proced Online 2018; 20: 5.

[25] Thomas DD and Wink DA. NOS2 as an emergent player in progression of cancer. Antioxid Redox Signal 2017; 26: 963-5.

[26] De Oliveira GA, Cheng RYS, Ridnour LA, Basudhar D, Somasundaram V, McVicar DW, Monteiro HP and Wink DA. Inducible nitric oxide synthase in the carcinogenesis of gastrointestinal cancers. Antioxid Redox Signal 2017; 26: 1059-77.

[27] Ekmekcioglu S, Grimm EA and Roszik J. Targeting iNOS to increase efficacy of immunotherapies. Hum Vaccin Immunother 2017; 13: 1105-8.

[28] O'Donnell JS, Madore J, Li XY and Smyth MJ. Tumor intrinsic and extrinsic immune functions of CD155. Semin Cancer Biol 2020; 65: 189-96.

[29] Yu X, Harden K, Gonzalez LC, Francesco M, Chiang E, Irving B, Tom I, Ivelja S, Refino CJ, Clark H, Eaton D and Grogan JL. The surface protein TIGIT suppresses T cell activation by promoting the generation of mature immunoregulatory dendritic cells. Nat Immunol 2009; 10: 48-57.

[30] Wu B, Zhong C, Lang Q, Liang Z, Zhang Y, Zhao X, Yu Y, Zhang H, Xu F and Tian Y. Poliovirus receptor (PVR)-like protein cosignaling network: new opportunities for cancer immunotherapy. J Exp Clin Cancer Res 2021; 40: 267.

[31] Zhou X, Du J, Wang H, Chen C, Jiao L, Cheng X, Zhou X, Chen S, Gou S, Zhao W, Zhai W, Chen J and Gao Y. Repositioning liothyronine for cancer immunotherapy by blocking the interaction of immune checkpoint TIGIT/PVR. Cell Commun Signal 2020; 18: 142.

[32] Gorvel L and Olive D. Targeting the "PVR-TIGIT axis" with immune checkpoint therapies. F1000Res 2020; 9: F1000 Faculty Rev-354.

[33] Bolandi N, Derakhshani A, Hemmat N, Baghbanzadeh A, Asadzadeh Z, Afrashteh Nour M, Brunetti O, Bernardini R, Silvestris N and Baradaran B. The positive and negative immunoregulatory role of B7 family: promising novel targets in gastric cancer treatment. Int J Mol Sci 2021; 22: 10719.

[34] Rahbar R, Lin A, Ghazarian M, Yau HL, Paramathas S, Lang PA, Schildknecht A, Elford AR, Garcia-Batres C, Martin B, Berman HK, Leong WL, McCready DR, Reedijk M, Done SJ, Miller N, Youngson B, Suh WK, Mak TW and Ohashi PS. B7-H4 expression by nonhematopoietic cells in the tumor microenvironment promotes antitumor immunity. Cancer Immunol Res 2015; 3: 184-95.

[35] Choi IH, Zhu G, Sica GL, Strome SE, Cheville JC, Lau JS, Zhu Y, Flies DB, Tamada K and Chen L. Genomic organization and expression analysis of B7-H4, an immune inhibitory molecule of the B7 family. J Immunol 2003; 171: 4650-4.

[36] Dangaj D, Lanitis E, Zhao A, Joshi S, Cheng Y, Sandaltzopoulos R, Ra HJ, Danet-Desnoyers G, Powell DJ Jr and Scholler N. Novel recombinant human b7-h4 antibodies overcome tumoral immune escape to potentiate T-cell antitumor responses. Cancer Res 2013; 73: 4820-9.

[37] Garon EB, Rizvi NA, Hui R, Leighl N, Balmanoukian AS, Eder JP, Patnaik A, Aggarwal C, Gubens M, Horn L, Carcereny E, Ahn MJ, Felip E, Lee JS, Hellmann MD, Hamid O, Goldman JW, Soria JC, Dolled-Filhart M, Rutledge RZ, Zhang J, Lunceford JK, Rangwala R, Lubiniecki GM, Roach C, Emancipator K and Gandhi L; KEYNOTE-001 Investigators. Pembrolizumab for the treatment of non-small-cell lung cancer. N Engl J Med 2015; 372: 2018-28.

[38] Qin S, Xu L, Yi M, Yu S, Wu K and Luo S. Novel immune checkpoint targets: moving beyond PD-1 and CTLA-4. Mol Cancer 2019; 18: 155.

[39] Tawbi HA, Schadendorf D, Lipson EJ, Ascierto PA, Matamala L, Castillo Gutiérrez E, Rutkowski P, Gogas HJ, Lao CD, De Menezes JJ, Dalle S, Arance A, Grob JJ, Srivastava S, Abaskharoun M, Hamilton M, Keidel S, Simonsen KL, Sobiesk AM, Li B, Hodi FS and Long GV; RELATIVITY-047 Investigators. Relatlimab and nivolumab versus nivolumab in untreated advanced melanoma. N Engl J Med 2022; 386: 24-34.

Supplementary Table 1. Overview of immune checkpoint markers

Immune checkpoint markers	Molecular features	Association with cancer immunity	Examples of the drugs and their mechanism	Supplementary Reference
ADORA2A	ADORA2A (adenosine A2A receptor) is expressed on variety of immune cells especially on T cells. When extracellular adenosine binds to ADORA2A, intracellular signaling that upregulate inhibitory cytokines and inhibitory receptors.	In-vivo experiment showed that inhibition of ADORA2A can upregulate cancer immunity.	Ciforadenant: oral antagonist of ADORA2A. Imaradenant: oral antagonist of ADORA2A.	[1, 2]
BTLA	BTLA (B- and T-lymphocyte attenuator) is mainly expressed on T-cells, but also on B-cells and dendritic cells. The main ligand of BTLA is herpes virus entry mediator (HVEM) The interaction between BTLA and HVEM leads to immunosuppression despite opposite effects have been described.	Increased expression of BTLA in tumor is reported to be associated with decreased anti-tumor immunity. BTLA neutralizing antibody showed better tumor control in mice.	BTLA neutralizing antibody.	[3]
CD276	CD276 (also known as B7-H3) is a tumor antigen expressed on variety of various cancer cells. Although CD276 binds to CD8+ T-cell trem-like transcript 2 in mice, the molecule to bind CD276 has not been identified in human.	CD276 in tumor is correlated with aggressive biology, low tumor infiltrating T-cells, more tumor infiltrating regulatory T-cells, and suppression of NK-cell-mediated glioma cell lysis.	Omburtamab: humanized monoclonal antibody toward CD276. MGC018: antibody drug conjugates with duocarmycin. CAR-T.	[4]
CTLA4	Cytotoxic T-lymphocyte-associated protein 4 (CTLA4) is expressed on activated T cells. CD80 and CD86 on antigen presenting cells (APC) are the ligands of CTLA4. Immune-inhibitory mechanism of CTLA4 is still unclear but it may remove CD80 and CD86 from APC so that they do not bind to immune-stimulatory receptors and modulate cellular motility.	Blockade of CTLA-4 using monoclonal antibody has been shown to bring about durable tumor regression in several clinical trials.	Ipilimumab: fully human IgG1 monoclonal antibody targeting CTLA4. Tremelimumab: fully human IgG2 monoclonal antibody targeting CTLA4.	[5]
IDO1	Indoleamine-pyrrole 2,3-dioxygenase 1 (IDO1) is an enzyme expressed in various normal tissues but highly expressed in cancer cells. The immune checkpoint mechanism of IDO1 is unclear, but it decreases tryptophane and produces kynurenine, leading to cell cycle arrest of neighboring T cells.	Some evidence exist that increased IDO1 expression in tumor is associated with poorer prognosis.	Epacadostat: selective, Trp competitive IDO1 inhibitor. Navoximod: Trp non-competitive IDO1 inhibitor. BMS-986205: irreversible inhibitor of IDO1.	[6, 7]
IDO2	Indoleamine-pyrrole 2,3-dioxygenase 2 (IDO2) is a paralog of IDO1. Compared to IDO1, tryptophane catabolic activity of IDO2 is minimal and main function of IDO2 is unclear.	The overexpression of IDO2 is reported in various types of cancer. IDO2 knock-out mice, especially female mice, demonstrated less risk to develop pancreatic ductal adenocarcinoma.	Diaryl hydroxylamines: dual inhibitor of IDO1 and IDO2.	[8]
LAG3	Lymphocyte activation gene 3 (LAG3) is a cell surface molecule on activated T cells, NK cells, and B cells. LAG3 is a main ligand of MHC class II and Fibrinogen-like protein 1 and contributes to immune tolerance.	LAG3 is upregulated in various types of cancer.	Relatlimab: human IgG4 LAG-3-blocking antibody (combination with nivolumab was approved for unresectable or metastatic melanoma by FDA in 2022).	[9, 10]
NOS2	Nitric oxide synthase 2 (NOS2) is an enzyme expressed in epithelial cells of the liver, lung, and bone marrow. NOS2 plays a role in innate immunity and deficiency is associated with susceptibility to certain viral infections.	Aberrant expression of NOS2 has been reported in some cancers. Overexpression of NOS2 may contribute to resistance to immunotherapy in several types of cancer.	Currently no medication targeting NOS2 is available.	[11]
PD-1	Programmed cell death protein 1 (PD-1) is a protein expressed on T cells and pro B cells and macrophages. The ligands of PD-1 are programmed death ligand 1 (PD-L1) and 2 (PD-L2). Binding to PD-L1 or PD-L2, PD-1 induces apoptosis of antigen specific T cells and also reduces apoptosis of regulatory T cells.	PD-L1, a ligand of PD-1 is expressed in various types of cancer. Many clinical trials of monoclonal antibodies to PD-1 showed significant anti-tumor effect and four PD-1 inhibitors have been approved as cancer therapies.	Pembrolizumab: humanized antibody blocking PD-1. Nivolumab: fully human antibody blocking PD-1. Cemiplimab: humanized, hinge-stabilized, IgG4K monoclonal antibody blocking PD-1. Dostarlimab: humanized IgG4 monoclonal antibody blocking PD-1.	[12]

PD-L1	Programmed death-ligand 1 (PD-L1) is a ligand of PD-1. PD-L1 is expressed on various immune cells, vascular endothelial cells and many types of malignant cells. When PD-L1 binds to PD-1, it induces apoptosis of antigen specific T cells.	PD-L1, a ligand of PD-1 is expressed in various types of cancer. Many clinical trials of monoclonal antibodies to PD-L1 showed significant anti-tumor effect and four PD-L1 inhibitors have been approved as cancer therapies.	Atezolizumab: fully human IgG1 antibody targeting PD-L1. Avelumab: fully human IgG1 antibody targeting PD-L1. Durvalumab: fully human IgG1 antibody targeting PD-L1.	[13]
PD-L2	Programmed death protein 1 ligand 2 (PD-L2) is a ligand of PD-1. PD-L2 is normally expressed on the antigen presenting cells, but also expressed in variety of tissues including malignancy. PD-L2 plays a role in immune tolerance cooperatively with PD-1 and PD-L1.	The role of PD-L2 in cancer immunity is not as established as that of PD-L1. PD-L2 is reported to be an independent response marker to immunotherapy.	There is no agent available that specifically inhibit PD-L2. However, PD-1 inhibitor inhibits both PD-1 and PD-L1 binding and PD-1 and PD-L2 binding.	[14]
PVR	Poliovirus receptor (PVR) is a transmembrane glycoprotein usually working to establish an inter-cellular adhesion with epithelial cells. PVR like protein co-signaling network plays a role in regulation of NK cells and T cells.	In vivo evidence suggests higher PVR expression is associated with tumor growth.	There is currently no medication to inhibit PVR.	[15]
TIGIT	T cell immunoreceptor with Ig and ITIM domains (TIGIT) is a transmembrane glycoprotein receptor expressed by T cells and NK cells. TIGIT is a part of PVR like protein co-signaling network and can bind to PVR and CD112.	In vitro, vivo, and clinical study demonstrated the efficacy of TIGIT blockade promoting NK cell mediated anti-tumor reactivity.	Tiragolumab: fully human monoclonal IgG1 antibody blocking TIGIT-PVR interaction. Vibostolimab: humanized monoclonal IgG1 antibody targeting TIGIT.	[16]
TIM3	T-cell immunoglobulin and mucin-domain containing-3 (TIM3) is a transmembrane protein expressed on a variety of immune cells including T cells. There are several ligands of TIM3, including galectin-9, PtdSer, HMGB1, CEACAM1. The interactions of TIM3 and its ligand lead to inactivation, anergy and apoptosis of T cells.	TIM3 expression is upregulated in various cancers. In vivo evidence suggests that co-blockade of TIM3 and PD-1 can result in tumor regression and improve anticancer T cell responses in advanced cancers.	Sabatolimab: humanized IgG4 antibody targeting TIM3. Cobolimab: humanized IgG4 antibody targeting TIM3.	[17]
VISTA	V-domain Ig suppressor of T cell activation (VISTA) is a transmembrane protein expressed on myeloid cells, lymphocytes and tumor cells. VISTA serves as a ligand and a receptor. VISTA can bind with P-selectin glycoprotein ligand-1 or V-Set and immunoglobulin domain containing 3 and inhibit T cell proliferation and cytokine production.	VISTA is overexpressed in various types of cancer compared to healthy tissues.	CA-170: tripeptide small molecule antagonist of VISTA. CI-8993: human IgG1 kappa monoclonal antibody designed to antagonize the VISTA.	[18]
VTCN1	V-set domain-containing T-cell activation inhibitor 1 (VTCN1) is a transmembrane protein expressed on various normal cells, immune cells and tumors. The receptor of VTCN1 is not found yet.	Overexpression of VTCN1 in various types of cancer has been reported. VTCN1 plays a role in different states of tumorigenesis, including cell proliferation, invasion, metastasis, anti-apoptosis.	There is currently no medication to inhibit VTCN1.	[19]

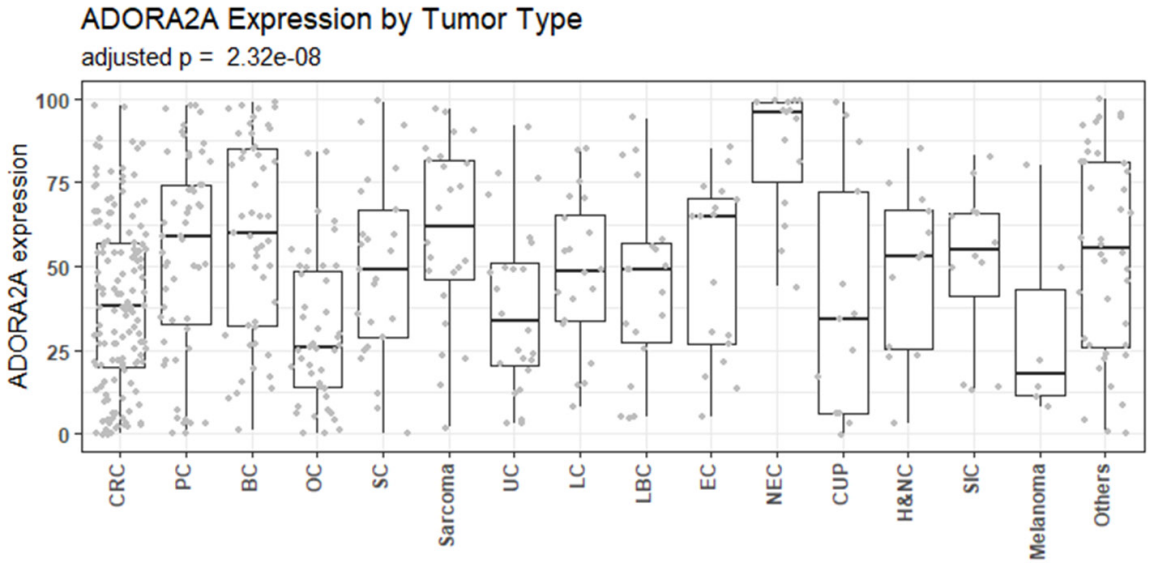
ADORA2A Expression by Tumor Type
adjusted p = 2.32e-08
ADORA2A expression
100
75
50
25
0
CRC
PC
BC
OC
SC
Sarcoma
UC
LC
LBC
EC
NEC
CUP
H&NC
SIC
Melanoma
Others

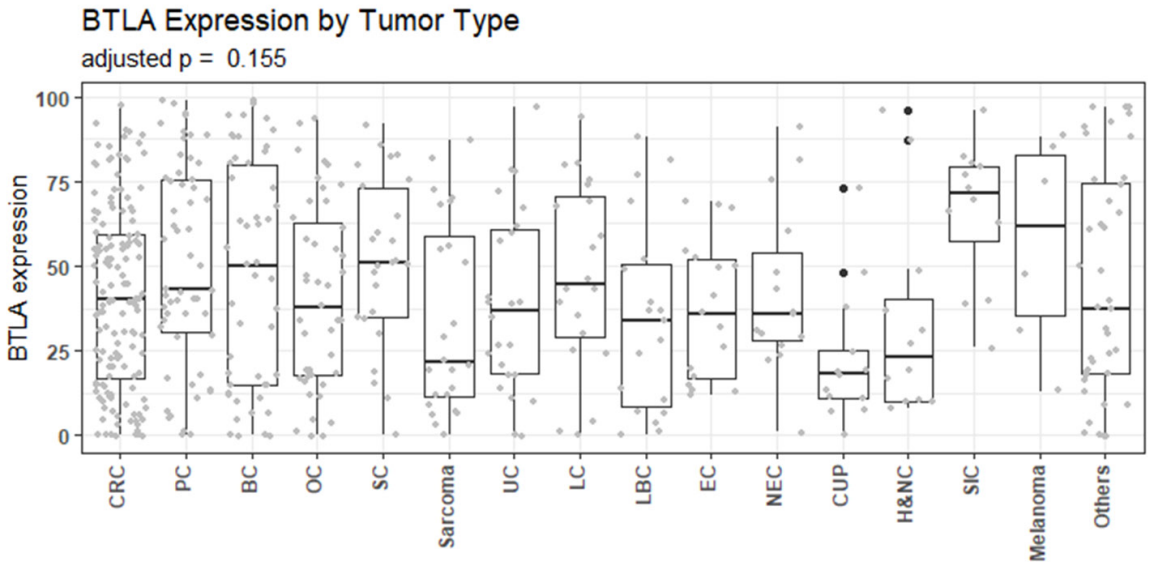
BTLA Expression by Tumor Type
adjusted p = 0.155
BTLA expression
100
75
50
25
0
CRC
PC
BC
OC
SC
Sarcoma
UC
LC
LBC
EC
NEC
CUP
H&NC
SIC
Melanoma
Others

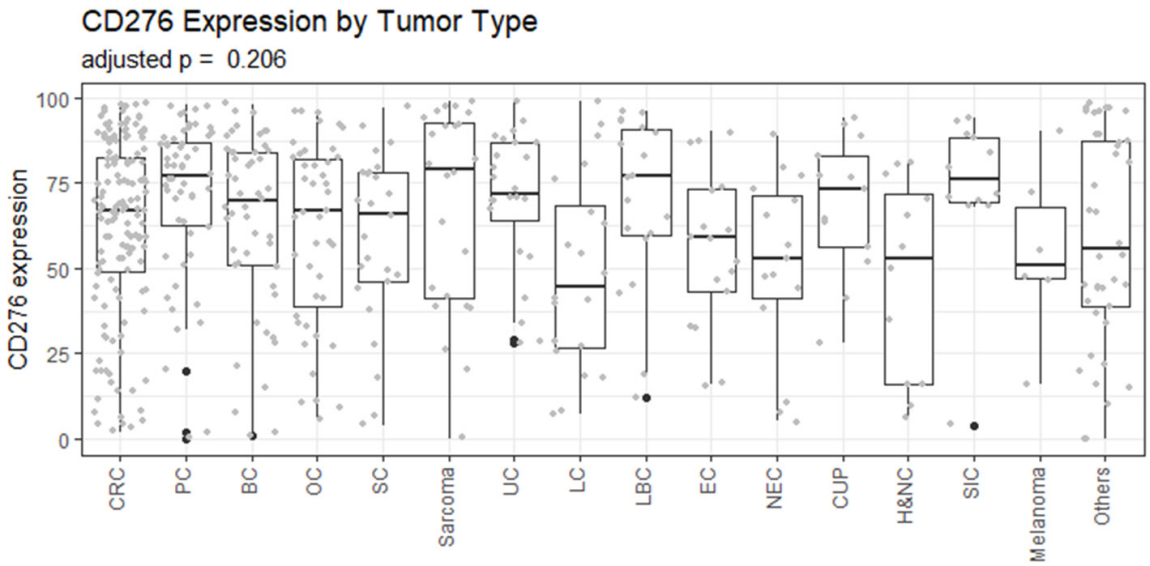
CD276 Expression by Tumor Type
adjusted p = 0.206
CD276 expression
100
75
50
25
0
CRC
PC
BC
OC
SC
Sarcoma
UC
LC
LBC
EC
NEC
CUP
H&NC
SIC
Melanoma
Others

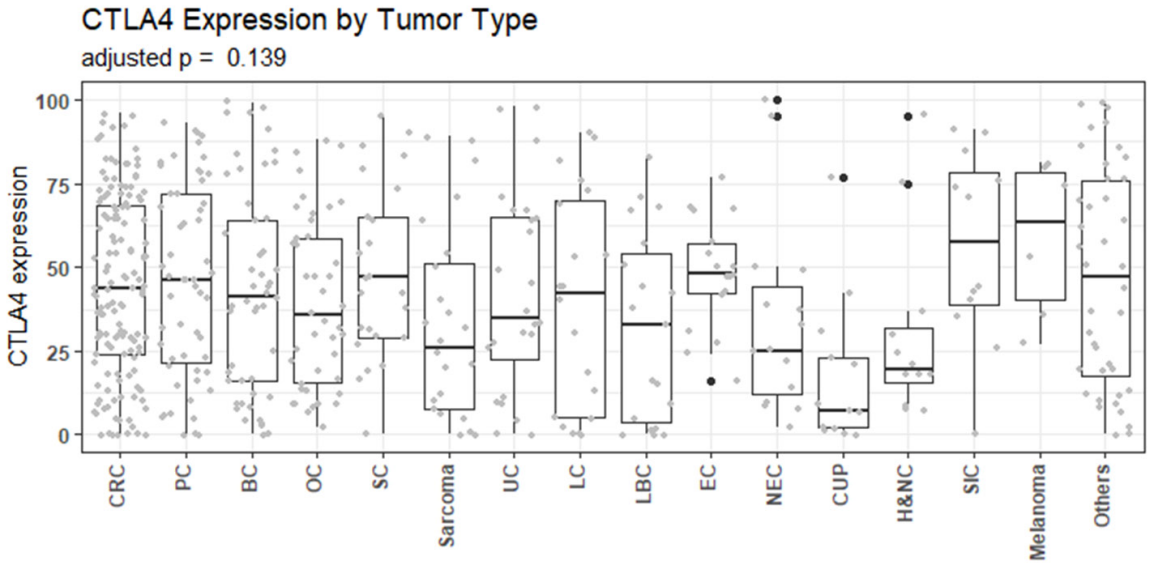
CTLA4 Expression by Tumor Type
adjusted p = 0.139
CTLA4 expression
100
75
50
25
0
CRC
PC
BC
OC
SC
Sarcoma
UC
LC
LBC
EC
NEC
CUP
H&NC
SIC
Melanoma
Others

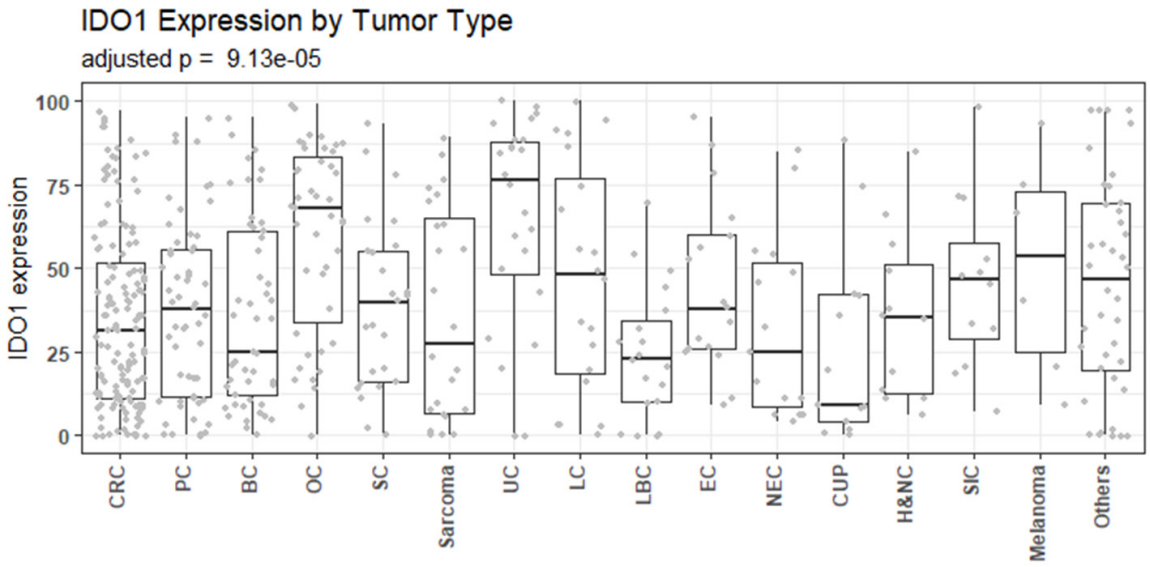
IDO1 Expression by Tumor Type
adjusted p = 9.13e-05
IDO1 expression
100
75
50
25
0
CRC
PC
BC
OC
SC
Sarcoma
UC
LC
LBC
EC
NEC
CUP
H&NC
SIC
Melanoma
Others

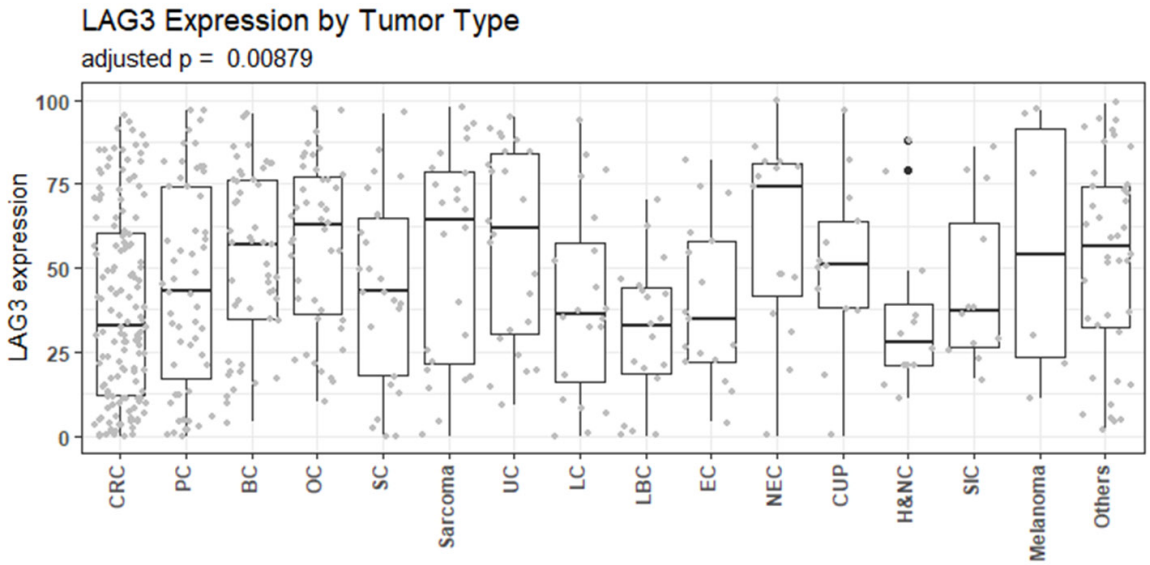
LAG3 Expression by Tumor Type
adjusted p = 0.00879
LAG3 expression
100
75
50
25
0
CRC
PC
BC
OC
SC
Sarcoma
UC
LC
LBC
EC
NEC
CUP
H&NC
SIC
Melanoma
Others

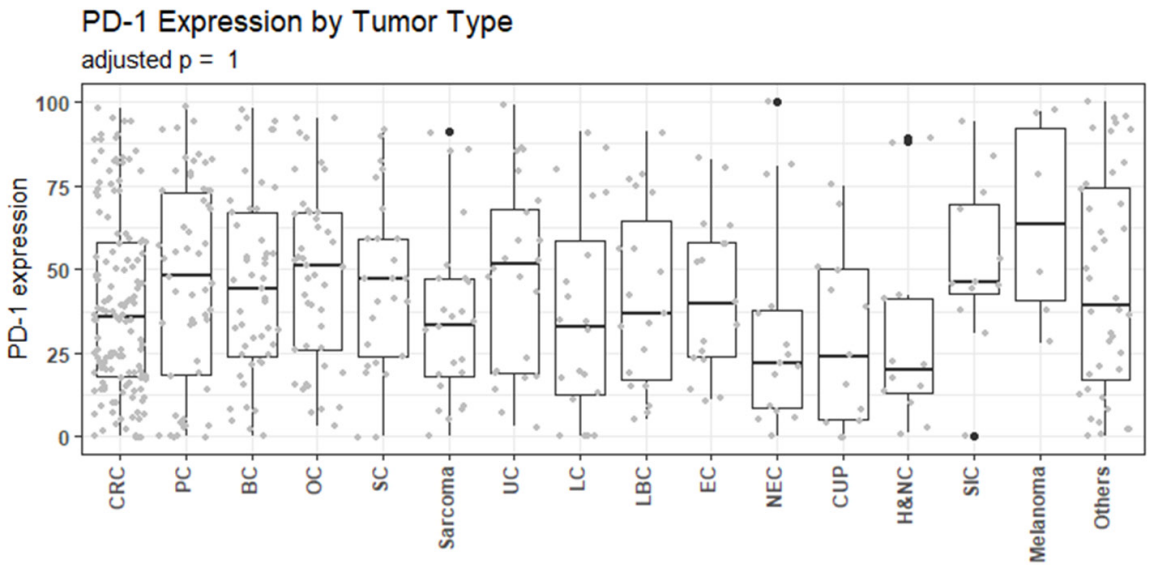
PD-1 Expression by Tumor Type
adjusted p = 1
PD-1 expression
100
75
50
25
0
CRC
PC
BC
OC
SC
Sarcoma
UC
LC
LBC
EC
NEC
CUP
H&NC
SIC
Melanoma
Others

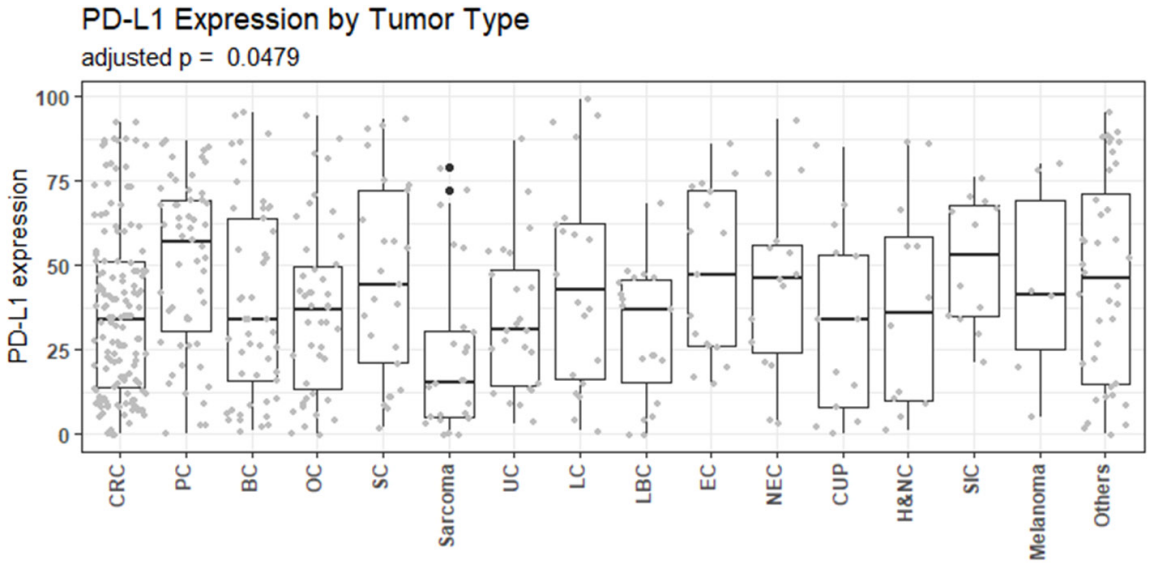
PD-L1 Expression by Tumor Type
adjusted p = 0.0479
PD-L1 expression
100
75
50
25
0
CRC
PC
BC
OC
SC
Sarcoma
UC
LC
LBC
EC
NEC
CUP
H&NC
SIC
Melanoma
Others

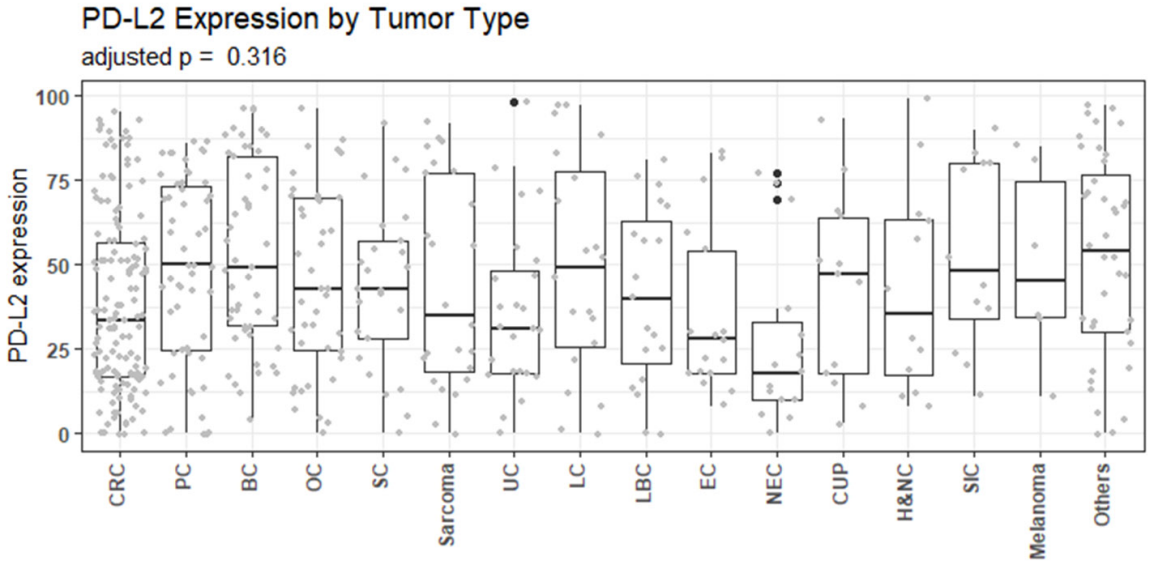
PD-L2 Expression by Tumor Type
adjusted p = 0.316
PD-L2 expression
100
75
50
25
0
CRC
PC
BC
OC
SC
Sarcoma
UC
LC
LBC
EC
NEC
CUP
H&NC
SIC
Melanoma
Others

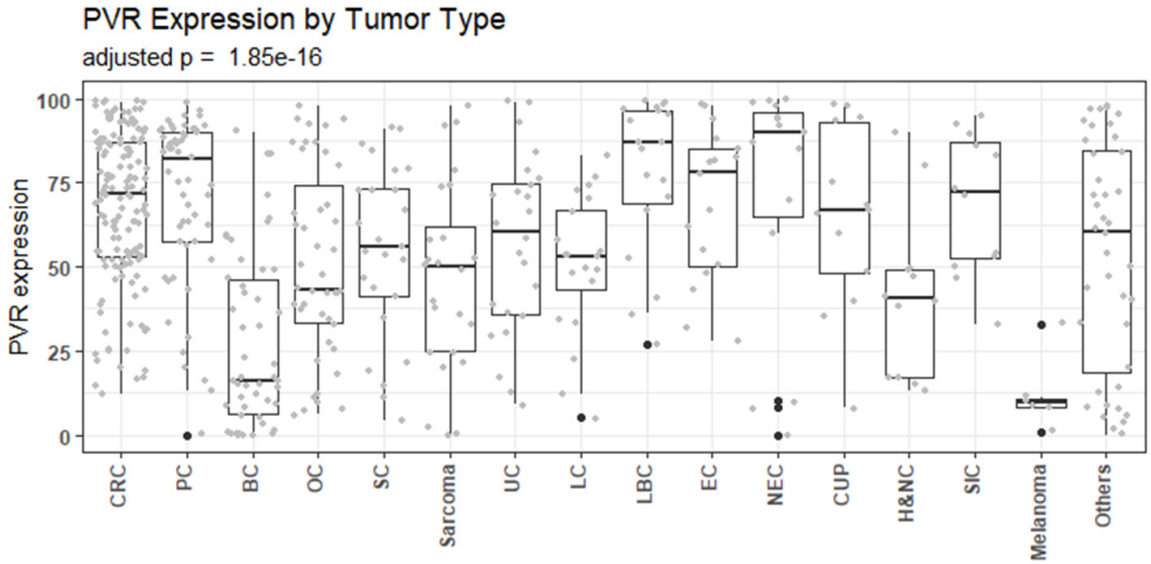
PVR Expression by Tumor Type
adjusted p = 1.85e-16
PVR expression
100
75
50
25
0
CRC
PC
BC
OC
SC
Sarcoma
UC
LC
LBC
EC
NEC
CUP
H&NC
SIC
Melanoma
Others

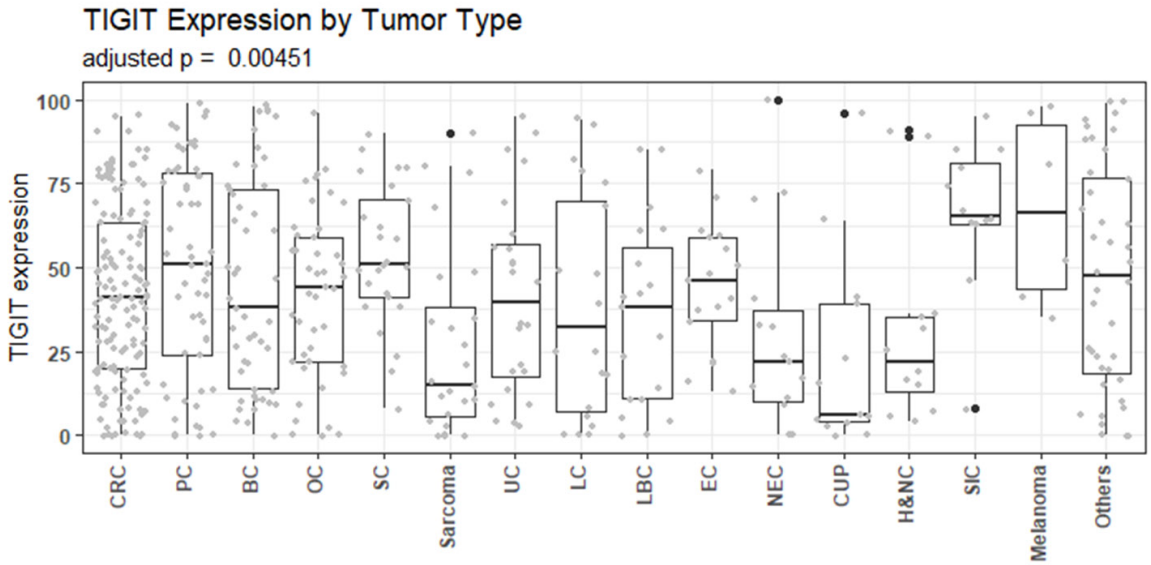
TIGIT Expression by Tumor Type
adjusted p = 0.00451
TIGIT expression
100
75
50
25
0
CRC
PC
BC
OC
SC
Sarcoma
UC
LC
LBC
EC
NEC
CUP
H&NC
SIC
Melanoma
Others

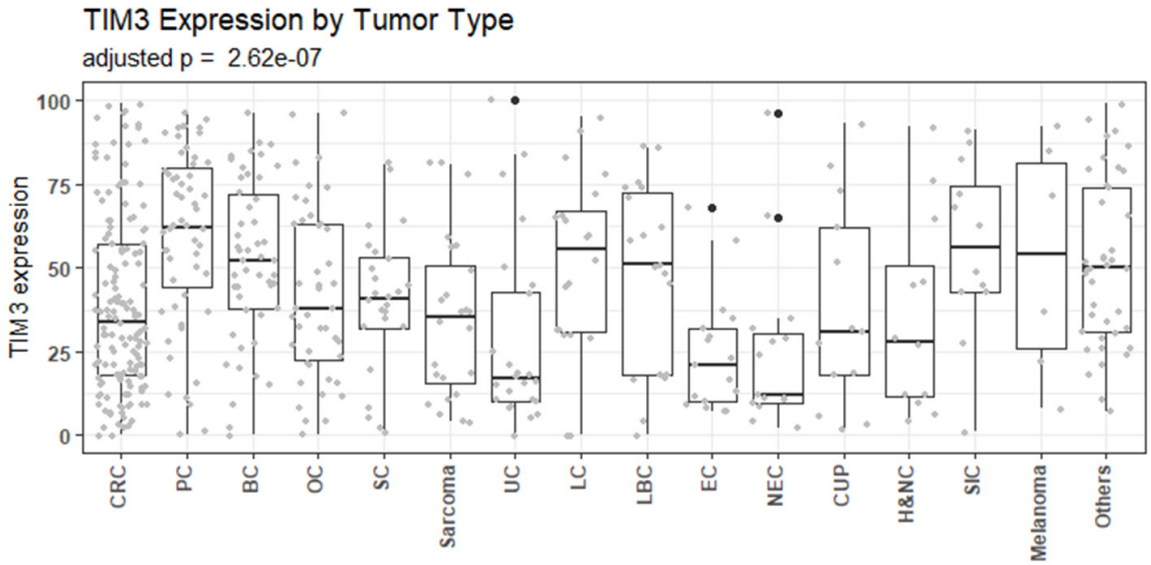
TIM3 Expression by Tumor Type
adjusted p = 2.62e-07
TIM3 expression
100
75
50
25
0
CRC
PC
BC
OC
SC
Sarcoma
UC
LC
LBC
EC
NEC
CUP
H&NC
SIC
Melanoma
Others

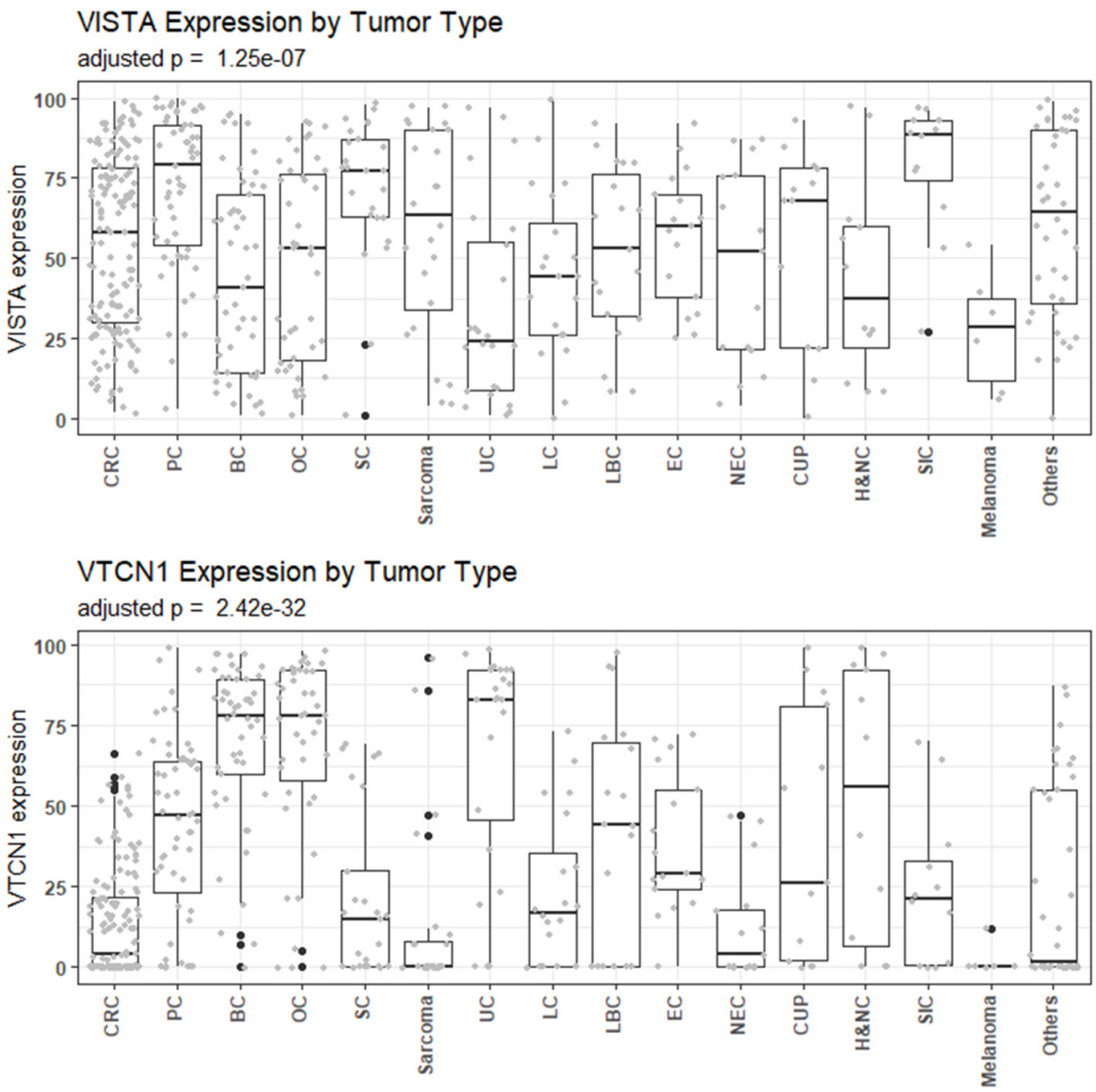

Supplementary Figure 1. Box plots for the expression of checkpoint markers. Each box represents the middle 50% of scores for the group. The bottom of the box represents the first quartile, and the top represents the third quartile. The thick line dividing the box into two parts means the median. The upper whisker extends to the largest value no further than 1.5 times of inter-quartile range from the third quartile. The lower whisker extends to the smallest value no further than 1.5 times of inter-quartile range from the first quartile. Any values outside the scope of the box and the whiskers are regarded as outliers and demonstrated by solid dots. Gray dots represent all values in the entire cohort. *P*-values were calculated by the Kruskal-Wallis test with Bonferroni correction for the multiple comparisons for the 16 genes. ADORA2A, IDO1, LAG3, PD-L1, PVR, TIGIT, TIM3, VISTA and VTCN1 showed significant difference between cancer types (See also **Figure 3** for information about IDO2 and NOS2). Abbreviations: BC: breast cancer, CRC: colorectal cancer, CUP: cancer of unknown primary, EC: esophageal cancer, H&NC: head and neck cancer, LBC: liver and bile duct cancer, LC: lung cancer, NEC: neuroendocrine cancer, OC: ovarian cancer, PC: pancreatic cancer, SC: stomach cancer, SIC: small intestine cancer, UC: uterine cancer.

Supplementary Table 2. The silhouette scores and standard deviation for random clusters of cancer types (See also **Figure 4**)

Random Count	Items	Attempt 1	Attempt 2	Attempt 3	Attempt 4
1000 Time	Mean	-0.1036	-0.1023	-0.1034	-0.1032
	SD	0.0149	0.0154	0.0152	0.0154
10000 Time	Mean	-0.1031	-0.1031	-0.1031	-0.1031
	SD	0.0154	0.0154	0.0153	0.0154
100000 time	Mean	-0.1031	-0.1030	-0.1030	-0.1030
	SD	0.0154	0.0154	0.0153	0.0154

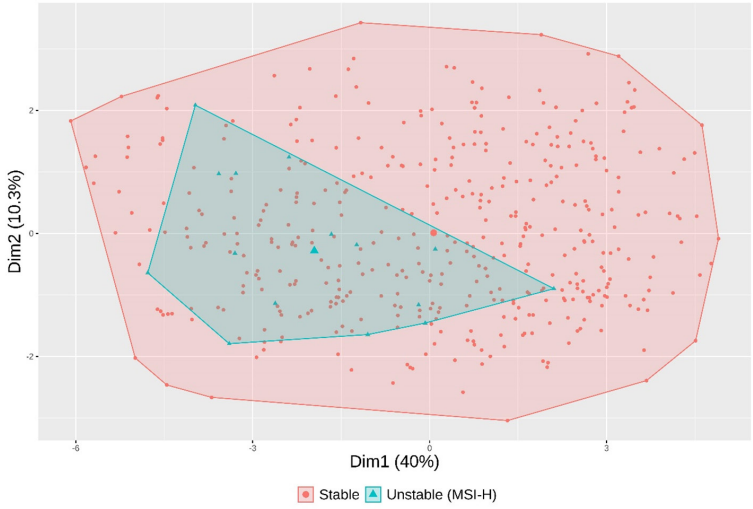

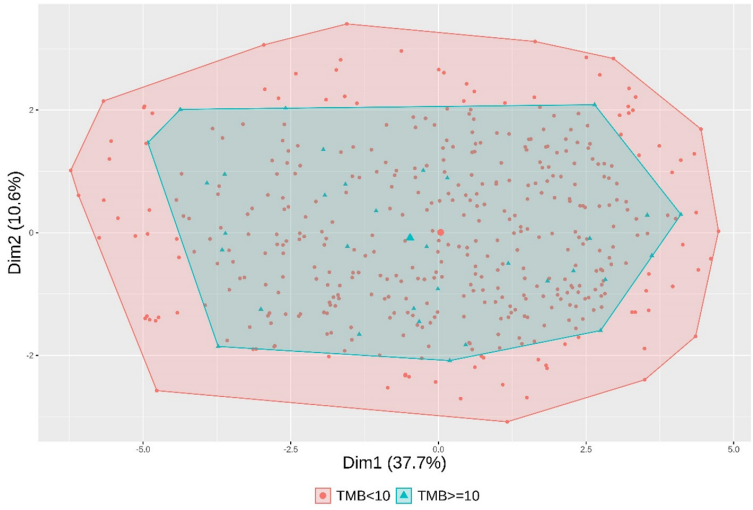

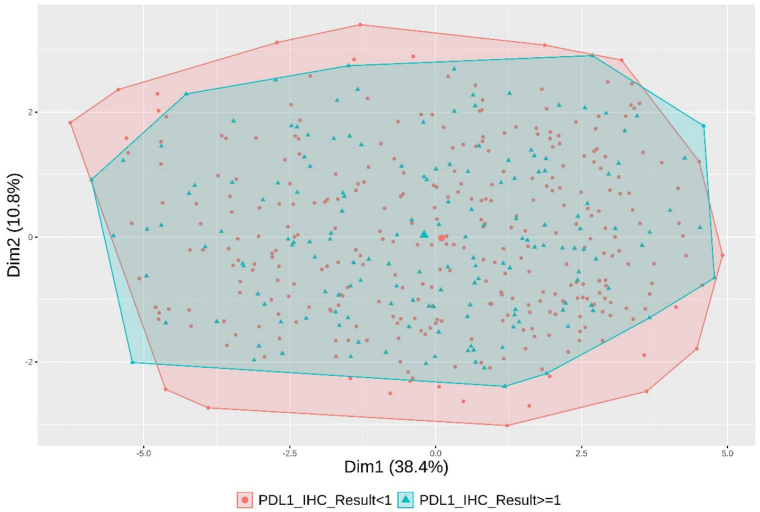

Supplementary Figure 2. The cluster of plots of dataset for the selected 16 checkpoint RNA expression based on microsatellite status, tumor mutational burden and PD-L1 immunohistochemistry using principal component analysis. The cluster of plots of dataset the selected 16 checkpoint genes (see Supplementary Table 1) which were assessed for RNA expression level based on MSI, TMB and PD-L1 IHC using principal component analysis. The cluster assignment is made based on MSI, TMB and PD-L1 IHC. To test this prediction, we first use principal component analysis to allow 2D representation of 16-dimensional data (considering each gene a dimension). Examining the distribution of values in the 1st and 2nd dimensions with each parameter shown in a distinct color. From this plot, it does not seem that there is a clear distinction between MSI, TMB and PD-L1 IHC status in the expression of the 16 checkpoint genes.

Supplementary References

[1] Leone RD, Lo YC and Powell JD. A2aR antagonists: next generation checkpoint blockade for cancer immunotherapy. Comput Struct Biotechnol J 2015; 13: 265-72.

[2] Sitkovsky MV, Kjaergaard J, Lukashev D and Ohta A. Hypoxia-adenosinergic immunosuppression: tumor protection by T regulatory cells and cancerous tissue hypoxia. Clin Cancer Res 2008; 14: 5947-52.

[3] Ning Z, Liu K and Xiong H. Roles of BTLA in immunity and immune disorders. Front Immunol 2021; 12: 654960.

[4] Kontos F, Michelakos T, Kurokawa T, Sadagopan A, Schwab JH, Ferrone CR and Ferrone S. B7-H3: an attractive target for antibody-based immunotherapy. Clin Cancer Res 2021; 27: 1227-35.

[5] Ribas A and Wolchok JD. Cancer immunotherapy using checkpoint blockade. Science 2018; 359: 1350-5.

[6] Zhai L, Ladomersky E, Lenzen A, Nguyen B, Patel R, Lauing KL, Wu M and Wainwright DA. IDO1 in cancer: a Gemini of immune checkpoints. Cell Mol Immunol 2018; 15: 447-57.

[7] Prendergast GC, Malachowski WP, DuHadaway JB and Muller AJ. Discovery of IDO1 inhibitors: from bench to bedside. Cancer Res 2017; 77: 6795-811.

[8] Mondanelli G, Mandarano M, Belladonna ML, Suvieri C, Pelliccia C, Bellezza G, Sidoni A, Carvalho A, Grohmann U and Volpi C. Current challenges for IDO2 as target in cancer immunotherapy. Front Immunol 2021; 12: 679953.

[9] Shi AP, Tang XY, Xiong YL, Zheng KF, Liu YJ, Shi XG, Lv Y, Jiang T, Ma N and Zhao JB. Immune checkpoint LAG3 and its ligand FGL1 in cancer. Front Immunol 2022; 12: 785091.

[10] Tawbi HA, Schadendorf D, Lipson EJ, Ascierto PA, Matamala L, Castillo Gutiérrez E, Rutkowski P, Gogas HJ, Lao CD, De Menezes JJ, Dalle S, Arance A, Grob JJ, Srivastava S, Abaskharoun M, Hamilton M, Keidel S, Simonsen KL, Sobiesk AM, Li B, Hodi FS and Long GV; RELATIVITY-047 Investigators. Relatlimab and nivolumab versus nivolumab in untreated advanced melanoma. N Engl J Med 2022; 386: 24-34.

[11] Ekmekcioglu S, Grimm EA and Roszik J. Targeting iNOS to increase efficacy of immunotherapies. Hum Vaccin Immunother 2017; 13: 1105-8.

[12] Chen W, Huang Y, Pan W, Xu M and Chen L. Strategies for developing PD-1 inhibitors and future directions. Biochem Pharmacol 2022; 202: 115113.

[13] Chang E, Pelosof L, Lemery S, Gong Y, Goldberg KB, Farrell AT, Keegan P, Veeraraghavan J, Wei G, Blumenthal GM, Amiri-Kordestani L, Singh H, Fashoyin-Aje L, Gormley N, Kluetz PG, Pazdur R, Beaver JA and Theoret MR. Systematic review of PD-1/PD-L1 inhibitors in oncology: from personalized medicine to public health. Oncologist 2021; 26: e1786-99.

[14] Yearley JH, Gibson C, Yu N, Moon C, Murphy E, Juco J, Lunceford J, Cheng J, Chow LQM, Seiwert TY, Handa M, Tomassini JE and McClanahan T. PD-L2 expression in human tumors: relevance to anti-PD-1 therapy in cancer. Clin Cancer Res 2017; 23: 3158-67.

[15] Wu B, Zhong C, Lang Q, Liang Z, Zhang Y, Zhao X, Yu Y, Zhang H, Xu F and Tian Y. Poliovirus receptor (PVR)-like protein cosignaling network: new opportunities for cancer immunotherapy. J Exp Clin Cancer Res 2021; 40: 267.

[16] Chauvin JM and Zarour HM. TIGIT in cancer immunotherapy. J Immunother Cancer 2020; 8: e000957.

[17] Wolf Y, Anderson AC and Kuchroo VK. TIM3 comes of age as an inhibitory receptor. Nat Rev Immunol 2020; 20: 173-85.

[18] Hosseinkhani N, Derakhshani A, Shadbad MA, Argentiero A, Racanelli V, Kazemi T, Mokhtarzadeh A, Brunetti O, Silvestris N and Baradaran B. The role of V-domain Ig suppressor of T cell activation (VISTA) in cancer therapy: lessons learned and the road ahead. Front Immunol 2021; 12: 676181.

[19] Wang JY and Wang WP. B7-H4, a promising target for immunotherapy. Cell Immunol 2020; 347: 104008.